

# More global randomness from less random local gates

Ryotaro Suzuki,<sup>1,\*</sup> Hosho Katsura,<sup>2</sup> Yosuke Mitsuhashi,<sup>3</sup> Tomohiro Soejima,<sup>4</sup> Jens Eisert,<sup>1</sup> and Nobuyuki Yoshioka<sup>5</sup>

<sup>1</sup>*Dahlem Center for Complex Quantum Systems, Freie Universität Berlin, Berlin 14195, Germany*

<sup>2</sup>*Department of Physics, The University of Tokyo, Tokyo 113-0033, Japan*

<sup>3</sup>*Department of Basic Science, The University of Tokyo, Tokyo 153-8902, Japan*

<sup>4</sup>*Department of Physics, Harvard University, Cambridge, MA 02138, USA*

<sup>5</sup>*International Center for Elementary Particle Physics, The University of Tokyo, Tokyo 113-0033, Japan*

Random circuits giving rise to unitary designs are key tools in quantum information science and many-body physics. In this work, we investigate a class of random quantum circuits with a specific gate structure. Within this framework, we prove that one-dimensional structured random circuits with non-Haar random local gates can exhibit substantially more global randomness compared to Haar random circuits with the same underlying circuit architecture. In particular, we derive all the exact eigenvalues and eigenvectors of the second-moment operators for these structured random circuits under a solvable condition, by establishing a link to the Kitaev chain, and show that their spectral gaps can exceed those of Haar random circuits. Our findings have applications in improving circuit depth bounds for randomized benchmarking and the generation of approximate unitary 2-designs from shallow random circuits.

Randomness is a ubiquitous concept across various subfields of physics, mathematics, and computer science. In particular, random unitary ensembles have a wealth of applications in quantum information processing, such as the error estimation via randomized benchmarking [1–4], providing computational advantage over classical computers [5–10], and verification of the state/process through quantum tomography [11–15]. Presumably the most commonly considered random unitaries, particularly in theoretical studies, is the global Haar random unitary ensemble, for which a unitary is chosen uniformly at random from the entire unitary group acting on the target system. However, while compelling mathematically, such a construction is notoriously impractical for systems of intermediate size. Consequently, genuine Haar randomness is often sacrificed for practicality by employing a sequence of *local* random circuits, which have their own wealth of applications in quantum science, such as modeling quantum chaotic many-body dynamics [16–23] and exploring the expressiveness of unitary operations [9, 23–33], as well as the applications for quantum information processing we have raised above.

An outstanding and practically relevant question that arises is: *Do local Haar random gates actually constitute the best randomizer to achieve global randomness?* Building on the seminal work by Brandão, Harrow, and Horodecki, which have shown that local random circuits can approximate  $n$ -qubit Haar random ensembles up to  $k$ -th order in  $O(nk^{10.5})$  depth under brick-wall architecture [25], there has been intensive pursuit to quantify how precisely the local random gate structure affects global randomness [21, 26–28, 34–40]. Most studies have assumed a fixed geometry of local random unitary gates, showing that a linear number of Haar random local gates in  $n$  can generate approximate unitary  $k$ -designs [26, 27, 36, 38, 41]; recent advances have achieved poly-logarithmic depth scaling with  $n$  through gluing of logarithmic-size random circuits [39, 40, 42]. More-

over, as a seminal result, a linear growth of approximate design orders has recently been achieved [28]. Crucially, however, existing works have predominantly assumed that local randomizers consist of local Haar random ensembles, or at least of a unitary subgroup. While being intuitive, it is far from clear whether this assumption is actually optimal or not. Furthermore, it is by far non-trivial to answer if there is any advantage at all to fixing certain gates to make the system more random. Similar questions have also been raised in Refs. [38, 39, 43] as open problems.

In this work, we answer the questions, by investigating models of random circuits with non-Haar local random gates, which does not form a group. We quantify the randomness by properties of the second-moment operators of structured random circuits, and we obtain all the eigenvalues and eigenvectors, not only the spectral gap, when they satisfy a solvable condition. As a consequence, we identify the counterintuitive result that random circuits consisting of structured random local gates can be substantially more random than those of Haar random local gates. We also discuss possible applications of our results, such as the reducing depth bounds for the randomized benchmarking by random quantum circuits [44] and the convergence rate to unitary 2-designs in shallow quantum circuits [39, 40, 42, 45].

*Setup for structured random circuits.* We investigate how the precise structure of random local gates affects the global randomness of an entire system, and to this end we introduce models of random circuits with non-Haar random gates. Concretely, we consider a random two-qudit gate generated by fixing a two-qudit gate  $u$  and sandwiching it by single-qudit Haar random gates acting on the inputs and the outputs, as shown in Fig. 1 (a), which we call  *$u$ -structured random gates*. A sequence of random gates specifies a probability distribution  $\nu$  in the unitary group, which we interchangeably refer to as the random circuit. We consider the following circuit architectures of one-dimensional structured random circuits consisting of qudits with local dimension  $d$ : (1)  *$u$ -structured local random circuit*  $\nu_u^L$ , where we pick up a neighboring pair of qudits uniformly at random and apply a  $u$ -structured random gate, which is illustrated in Fig. 1 (a), (2)  *$u$ -structured*

\* ryotaro.suzuki@fu-berlin.de

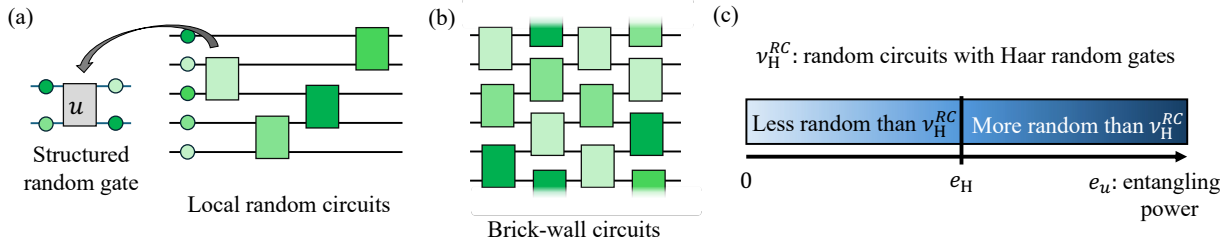


FIG. 1. Setup and main results. Structured random gates consist of a fixed two-qudit gate  $u$  and four Haar random single-qudit gates sandwiching it. We consider two models of random circuits, where structured random gates are applied in the (a) local random circuit architecture and (b) brick-wall circuit architecture, where the boxes are two-qudit gates and the balls are single-qudit Haar random unitaries. As stated in Theorem 1 and 2, we show that if the entangling power of a structured random gate is greater than that of Haar random gates, the structured random circuits satisfying a solvable condition are more random than Haar random circuits with the same architecture (c).

brick-wall random circuit  $\nu_u^B$ , where we apply staggered two layers of  $u$ -structured two-qudit gates on nearest neighbors, which is illustrated in Fig. 1 (b). For local random circuits, we apply single-qudit Haar random unitaries on the all qudits for technical convenience (Fig. 1 (a)) [46]. Likewise, we define local and brick-wall Haar random circuits by  $\nu_H^L$  and  $\nu_H^B$ , respectively, where we apply two-qudit Haar random gates in the corresponding architecture.

*Characterization of randomness.* A next step is to meaningfully quantify randomness. Here, we characterize randomness using the moment operator [24, 41]. Given a random circuit  $\nu$ , the second-moment operator is defined by  $M_\nu := \int U^{\otimes 2} \otimes \bar{U}^{\otimes 2} d\nu(U)$ , where  $\bar{U}$  is the complex conjugate of  $U$ . We denote moment operators for  $u$ -structured local and brick-wall random circuits in one step by  $M_{L,u}$  and  $M_{B,u}$ , respectively. For Haar random circuits, they are defined by replacing the subscript  $u$  by  $H$ . The moment operators of these circuits with  $t$  steps, or  $t$  depth, are obtained by multiplying them  $t$  times, namely  $(M_{a,u})^t$  for  $a = L, B$ . Since we apply single-qudit Haar random unitaries on all qudits in both architectures, and they are the projector onto the  $2^n$ -dimensional subspace  $\text{span}\{|I\rangle, |S\rangle\}^{\otimes n}$  [25], it is enough to consider  $M_{a,u}$  restricted to the subspace, for  $a = L, B$ . Later, we show the diagonalization results in this subspace. We write the eigenvalues of  $M_\nu$  in non-increasing order in absolute value  $|\lambda_1| \geq |\lambda_2| \geq \dots$ , where we have  $\lambda_i = 1$  for  $i = 1, 2$ . The largest eigenvalue is 1 and the eigenspace  $V_1$  is spanned by the  $n$ -fold vectorization of the identity (SWAP) gate  $|I\rangle$  ( $|S\rangle$ ) (see Sec. S2 in the Supplementary Material (SM) for details [47]).

The gap between the largest and second-largest eigenvalues of  $M_\nu$  in absolute value, which is  $1 - |\lambda_3|$ , is called the *spectral gap*, denoted by  $\Delta_\nu$ . The eigenvalues of  $M_\nu$  determine the convergence rate to unitary 2-designs [24, 25, 48, 49] (see Sec. S2 A in the SM [47]), where unitary  $k$ -designs are ensembles whose  $k$ -th moment agrees with that of global Haar random unitaries. Concretely, when the eigenvalues of  $M_\nu$  are small and hence its spectral gap is large, we have fast convergence to unitary 2-designs. We then formalize what “more randomness” means in two ways, where the former is based on the spectral gap and the latter is rooted in the entire property of second-moment operators.

**Definition 1** (More random with respect to spectral gaps). *Let  $\nu$  and  $\mu$  be probability distributions of random circuits. The distribution  $\nu$  is said to be more random than  $\mu$  if  $\Delta_\nu > \Delta_\mu$ .*

**Definition 2** (More random with respect to positivity). *When  $M_\nu$  and  $M_\mu$  are Hermitian operators,  $\nu$  is said to be more random with respect to positivity than  $\mu$  if the restriction of the operator  $M_\mu|_{V_1^\perp} - M_\nu|_{V_1^\perp}$  is a positive operator, where  $V_1^\perp$  is the orthogonal complement of  $V_1$ .*

The spectral gaps of the ensembles forming exact unitary 2-design are 1, and, therefore, they are the most random ensembles by Definition 1. We note that  $M_{L,u}$  is always Hermitian, since, as explained later, the operator is characterized by the entanglement properties of  $u$ , and they are invariant under the Hermitian conjugate. More generally, when the circuit architecture of  $\nu$  is invariant under the time reflection,  $M_\nu$  is Hermitian. We note if  $\lambda_3 \geq 0$  for both random circuits and  $\nu$  is more random with respect to positivity than  $\mu$ ,  $\nu$  is also more random than  $\mu$ , where this follows from Weyl’s monotonicity theorem [50]. Moreover, we remark on the definition based on positivity. One particular feature of Haar random unitaries is that an expectation value is highly concentrated around its mean value [51]. In this context, the bound on the second-moment implies the bound on the variance. Specifically, more randomness of  $\nu$  than  $\mu$  with respect to positivity implies that, for a state vector  $|\psi\rangle$ , the probability distribution of  $|\langle \psi | U | \psi \rangle|^2$  drawn  $U$  from a structured random circuit  $\nu$  is more concentrated around its mean value than that of another structured random circuit  $\mu$ . This kind of concentration bound has been used, for example, to prove the equilibration of random product states [52] and lower-bound the circuit complexity of the random unitary ensemble [20, 43].

*Entangling power and gate typicality.* When the fixed gate  $u$  is an entangling gate, the gate set becomes computationally universal, and eventually, random circuits converge to Haar random unitaries [25], while when  $u$  is not entangling, random circuits do not. This simple observation suggests that we can parameterize the randomness of structured random circuits by the entanglement property of  $u$ . In fact, we find that the second-moment operators of structured random circuits depend only on the entangling power  $e_u$  [53–56], which is the linear entanglement entropy of random product state applied

by  $u$ , and its complementary quantity  $g_u$ , called gate typically [54–56] (see Sec. S3 A in the SM for more details [47]). For two-qudit gate  $u$  for  $d = 2$  and  $d > 2$ , the entangling power can take all the value within  $0 \leq e_u \leq \frac{2}{3}$  and  $0 \leq e_u \leq 1$ , respectively. For two-qudit gate  $u$  with  $d \geq 2$ , the gate typicality takes  $0 \leq g_u \leq 1$ , where  $g_u = 1$  (0) if  $u$  is the two-qudit SWAP (identity) gate. In this sense, the gate typicality quantifies the extent to which a gate is close to the SWAP gate. For Haar random two-qudit unitary gates, the averaged entangling power and gate typicality are  $e_H = \frac{d^2-1}{d^2+1}$  and  $g_H = \frac{1}{2}$ , respectively. We note that the second-moment operators of  $u$ -structured random circuits satisfying  $e_u = e_H$  and  $g_u = g_H$  are equal to those of Haar random circuits.

*Solvable conditions.* We find the mapping from the moment operators of  $u$ -structured random circuits satisfying a solvable condition to free-fermion chains (see Sec. S5 in the SM [47]). In the general case of  $d \geq 2$ , the solvable condition is

$$\frac{e_u}{g_u} = \frac{e_H}{g_H}. \quad (1)$$

Under the solvable condition, we treat  $e_u$  as a free parameter and take  $g_u$  as a function of  $e_u$ . Clearly, the Haar values  $e_H$  and  $g_H$  satisfy the condition. We now turn to identifying the two-qubit gates that satisfy the condition: The two-qubit gates take the general form  $u = \exp\{-i(\alpha XX + \beta YY + \gamma ZZ)\}$ , up to single-qubit gates, where  $\alpha, \beta$ , and  $\gamma$  are real numbers and  $X, Y$ , and  $Z$  are Pauli matrices. Here, the choice of single-qubit gates is irrelevant to the moment operator, since structured random gates are sandwiched by single-qudit Haar random gates. With this parametrization, the solvable condition on the parameters is  $f(\alpha, \beta) + f(\beta, \gamma) + f(\gamma, \alpha) = 0$ , where  $f(x_1, x_2) = \sin^2 2x_1 (\cos^2 2x_2 - \frac{3}{5})$ . For example, when  $\alpha = \beta = \gamma$ , the solvable condition implies  $u = \exp\{-i\alpha(XX + YY + ZZ)\}$  with  $\cos 2\alpha = \pm\sqrt{3/5}$ . We remark that we can map the moment operators to free-fermion chains under the solvable condition, although the two-qubit gates are in general different from matchgates [57–59]. Intuitively, structured random circuits under the solvable condition are free-fermionic “on average”, while the individual instances are rather chaotic.

*Results for more randomness.* We show that  $u$ -structured random circuits can be more random than Haar random circuits, which are summarized as follows.

**Theorem 1** (More randomness with respect to spectral gaps). *Let  $u$  be a two-qudit gate which satisfies the solvable condition Eq. (1). Then,  $\nu_u^L$  and  $\nu_u^B$  are more random than  $\nu_H^L$  and  $\nu_H^B$ , respectively, if and only if  $e_u > e_H$ .*

**Theorem 2** (More randomness with respect to positivity). *For a general two-qudit gate  $u$ ,  $\nu_u^L$  is more random with respect to positivity than  $\nu_H^L$  if  $e_u > e_H$  and  $g_u > g_H$ .*

A crucial fact is that the entangling power of the Haar random two-qudit gates is not maximum, for example, in the two-qubit case,  $e_H = \frac{3}{5}$  while  $u$ -structured random gates can take the value at most  $e_u = \frac{2}{3}$ . From the above results, one might think that the spectral gap increases monotonically in  $e_u$  in

general. Under the solvable condition, it is correct for structured local random circuits, but not for structured brick-wall random circuits, as we have shown that the spectral gap of  $M_{B,u}$  can decrease with increasing  $e_u$  in the case of  $d = 3$  (see Sec. S4 B in the SM for details [47]). On the solvable line, we can diagonalize the second-moment operators and find that the  $t$ -depth  $u$ -structured local random circuits are more random than the  $t$ -depth local Haar random circuits if and only if  $e_u > e_H$ .

*Spectra of moment operators.* Next, we describe technical results on the exact eigenvalues of the moment operators. We assume that the qudit count  $n$  is even for technical convenience. The general case of  $n$  for  $\nu_u^L$  is discussed in Sec. S4 A in the SM [47]. To state these results, we define

$$K_p := \left\{ \frac{2m-p}{n} \pi \mid m = -\frac{n}{2} + 1, -\frac{n}{2} + 2, \dots, \frac{n}{2} \right\}, \quad (2)$$

for  $p \in \{0, 1\}$ , and label the eigenvalues by  $p$  and  $i_p = \{i_{p,k}\}_{k \in K_p}$  with  $i_{p,k} \in \{0, 1\}$  satisfying  $\sum_{k \in K_p} i_{p,k} = 0 \pmod{2}$ .

**Theorem 3** (Spectral values). *Let  $u$  be a two-qudit gate satisfying the solvable condition. Then, the eigenvalues of  $M_{L,u}$  are given by*

$$\lambda_{p,i_p} = 1 - \frac{1}{n} \sum_{k \in K_p} \epsilon_k i_{p,k}, \quad (3)$$

where  $\epsilon_k := \tilde{e}_u (1 - 2a_k)$ ,  $\tilde{e}_u := \frac{e_u}{e_H}$ , and  $a_k := \frac{d}{d^2+1} \cos k$ , and the eigenvalues of  $M_{B,u}$  are given by

$$\lambda_{p,i_p} = \prod_{k \in K_p} (\lambda_k)^{i_{p,k}}, \quad (4)$$

where  $\lambda_k := \left( a_k \tilde{e}_u + \sqrt{a_k^2 \tilde{e}_u^2 + 1 - \tilde{e}_u} \right)^2$ .

From the above result, we find that while the eigenvalues of  $M_{L,u}$  are always real, those of  $M_{B,u}$  can be non-real due to their non-Hermiticity. We note that

$$\lambda_{\pi-k} = \left( a_k \tilde{e}_u - \sqrt{a_k^2 \tilde{e}_u^2 + 1 - \tilde{e}_u} \right)^2 = \lambda_k^* \quad (5)$$

when  $a_k^2 \tilde{e}_u^2 + 1 - \tilde{e}_u < 0$ , where the eigenvalues come in complex conjugate pairs because  $M_{a,u}$  for  $a = L, B$  are real matrices. The spectral gaps of the moment operators are described in Sec. S4 in the SM [47].

*Proof sketch.* To begin with, we find that the moment operator of a structured local random circuit satisfying the solvable condition is mapped, via the Jordan-Wigner transformation, to the Kitaev chain [60]. The model is a free-fermionic model and hence exactly solvable. We then obtain all eigenvalues and eigenvectors of  $M_{L,u}$ . In particular, its eigenvalues and the spectral gap monotonically decrease and increase in  $e_u$ , respectively. With the observation that  $M_{L,u}|_{V_1^\perp}$  monotonically decreases with increasing  $e_u$  and  $g_u$ , we obtain the statements in the theorems for local random circuits.

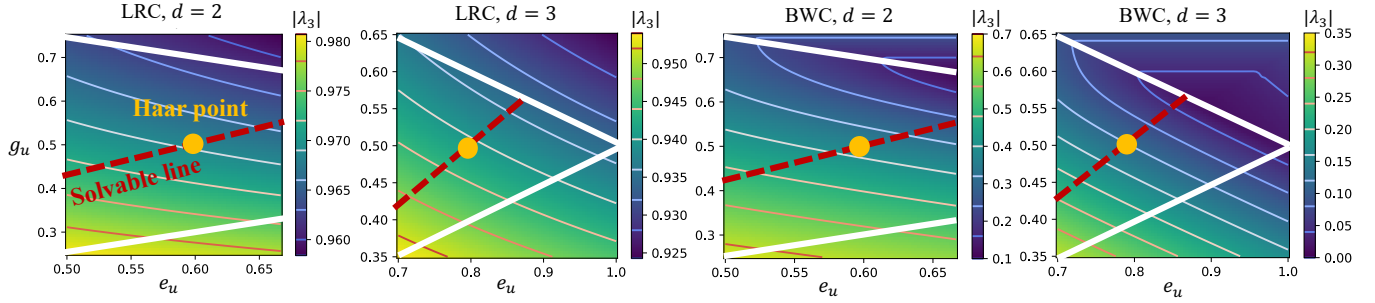


FIG. 2. Numerical results on  $|\lambda_3|$  of  $M_{L,u}$  (LRC) and  $M_{B,u}$  (BWC) for general  $e_u$  and  $g_u$  in qubit system ( $d = 2$ ) and qutrit system ( $d = 3$ ) in the case of  $n = 14$ . The x-axis and the y-axis refer to the entangling power  $e_u$  and the gate typicality  $g_u$ , respectively. We derive analytical solutions of them on the solvable lines (the broken red lines) satisfying the condition Eq. (1) in Theorem 3. At the Haar points (the orange dots), the second-moment operators of structured random circuits are equal to those of the Haar random circuits with the same architecture, and the points are on the solvable lines. Only the values between the thick white lines are feasible for  $e_u$  and  $g_u$ , as discussed in Sec. S3 A in the SM and also in Ref. [55].

For structured brick-wall random circuits, the moment operator is a product of two layers, where each layer is the tensor product of structured random gates. Under the solvable condition, by the free-fermion techniques, the diagonalization of the  $2^n \times 2^n$  matrix  $M_{B,u}$  reduces to the diagonalization of a family of  $4 \times 4$  matrices, and we obtain all the eigenvalues and eigenvectors of  $M_{B,u}$ . This yields the statements in the theorems for brick-wall circuits. The formal proofs can be found in Sec. S5 in the SM [47].

*Numerical results.* Along with the analytical solutions, we numerically calculate  $|\lambda_3| = 1 - \Delta_\nu$  of  $M_{L,u}$  and  $M_{B,u}$ , as shown in Fig. 2. The solvable condition is illustrated as the solvable lines there, and we confirm that the analytical results agree with the numerical results on the lines. Fig. 2 clearly illustrates our main statement that the spectral gap becomes larger than that of Haar points when  $e_u > e_H$ , where  $e_H = \frac{3}{5}$  for  $d = 2$  and  $e_H = \frac{4}{5}$  for  $d = 3$ . We find an interesting difference between local random circuits and brick-wall circuits as follows. In Figs. 2 (a) and (b) in the case of local random circuits, the spectral gap monotonically increases in  $g_u$ . However, in Figs. 2 (c) and (d) in the case of brick-wall random circuits, it reaches the minimal value, which is close to the line  $e_u = 2 - 2g_u$  (the thick upper white line shown in each plot), when we change  $g_u$  with fixed  $e_u$ . The two-qudit gates on the line  $e_u = 2 - 2g_u$  are the dual-unitary gates [55, 61–64], which serve as a toy model of chaotic dynamics. We leave it as an open problem to determine whether a dual-unitary gate achieves the largest spectral gap in the unitary gates with a given entangling power.

*Applications.* Simple as the modification, we suggest that it may open a number of compelling applications. We can apply the enhancement of randomness in terms of the second moment to the followings: (1) *Reduction of circuit depth for randomized benchmarking.* Randomized benchmarking (RB) [3] is a widely used technique for estimating the quality of quantum gates in quantum computers. There, random circuits serve as tools for assessing the error rate, known as the filtered RB, and the circuit depth for realizing it is upper-bounded by the inverse of the spectral gap of the second-moment op-

erator in a sufficiently large depth [44]. Combining it with our enhanced spectral gaps, we can improve the required circuit depth for the theoretically guaranteed RB. (2) *Improved bound on unitary 2-designs in shallow random circuits.* Unitary 2-designs have a range of applications, such as computational advantage [65, 66], quantum channel fidelity estimation [48], random coding [67, 68], and randomized measurement [13, 69]. Recently, Haar random circuits have been shown to form approximate unitary designs in depth  $\log n$  by the technique of gluing small random circuits [39, 40]. Since the structured random circuits can have better upper bounds on the depth generating approximate unitary 2-designs, combining it with the technique by gluing small structured random circuits, we can improve the approximate 2-design time. (3) *Exact result on quantum chaotic dynamics.* More physically motivated applications of our results manifest themselves by the connection between the second-moment operator and indicators of quantum chaos, such as *out-of-time ordered correlators* (OTOC) and the Rényi-2 operator entanglement entropy [18, 19, 23, 70]. Because we derive the eigenvalues and eigenvectors of the second-moment operators satisfying the solvable condition, one can obtain closed formulae for these indicators in structured random circuits satisfying the solvable condition.

*Discussion and conclusion.* In our work, we have given an affirmative answer to the fundamental problem of whether random circuits with non-Haar random gates can be more random than those with Haar random gates. The additional structure improves the convergence rate to a unitary 2-design ensemble, which will be particularly important when we use large-scale quantum computers. Since we have considered the second-moment, the Haar random single-qudit gates in the structured random gates can be replaced by any gates forming unitary 2-design locally, keeping our results the same. While we have focused on the diagonalization of moment operators in the main text, we also derive the bounds on the frame potential in structured random circuits, as shown in Sec. S6 in the SM [47]. Also, more randomness with respect to positivity in structured local random circuits is true for an arbitrary

spatial dimension (Sec. S5 A 1 in the SM [47]). We note that Ref. [29] has also derived the spectral gap of brick-wall Haar random circuits, and our result at the Haar point of  $e_u = e_H$  and  $g_u = g_H$  agrees with it. Also, the spectra of matchgate brick-wall circuits have been considered in Ref. [71], and we expect that our results on the diagonalization of brick-wall circuits are also applicable to matchgate unitary circuits.

Our results open up numerous opportunities for future work. It would be an interesting open problem to show more randomness of structured random circuits in terms of higher-moment operators, as well as other architectures, for example, higher dimensional brick-wall circuits. Other future directions are finer analyses of the applications we have discussed above. Also, investigating the randomness in Brownian Hamiltonian dynamics [35, 72] with an additional structure similar to this work would be a physically interesting direction. At the end of such a program stands an idea of how to best create randomness with smallest possible circuit complexity. We hope that this work helps to identify the fundamental limits of what notions of randomness one can actually achieve with reason-

able constraints on circuit complexity.

*Acknowledgements.* We thank Ingo Roth, Janek Denzler, Tomohiro Yamazaki, and Christian Bertoni for useful discussions. The Berlin team acknowledges the support by the German Federal Ministry for Education and Research (PhoQuant, DAQC, MuniQC-Atoms), the Munich Quantum Valley, the DFG (CRC 183 and FOR 2724), Berlin Quantum and the European Research Council (DebiQC). H. K. is supported by JSPS KAKENHI Grants No. JP23K25783, No. JP23K25790, and MEXT KAKENHI Grant-in-Aid for Transformative Research Areas A “Extreme Universe” (KAKENHI Grant No. JP21H05191). Y. M. is supported by JSPS KAKENHI Grant No. JP23KJ0421. N. Y. wishes to thank JST PRESTO No. JPMJPR2119, JST ASPIRE Grant Number JPMJAP2316, and the support from IBM Quantum. This research is funded in part by the Gordon and Betty Moore Foundation’s EPiQS Initiative, Grant GBMF8683 to T.S. This work was supported by JST Grant Number JPMJPF2221, JST ERATO Grant Number JPMJER2302, and JST CREST Grant Number JPMJCR2314, Japan.

# Supplementary Material: More global randomness from less random local gates

## S1. STRUCTURE OF SUPPLEMENTARY MATERIALS

This supplementary material is organized as follows. In Sec. S2, we give formal definitions of structured random circuits and review the properties of moment operators. We also introduce the Weingarten calculus, which is a key tool for analyzing moment operators. We then give a review of the entangling power and the gate typically in Sec. S3, and we parametrize the second-moment operators of structured random circuits by these quantities. In Sec. S4, we summarize the main results, including the exact diagonalization of the second-moment operators. In Sec. S5, we prove the main results by mapping the second-moment operators to free-fermion chains and the diagonalization of them. We also compute the frame-potential, which is another indicator of randomness, as shown in Sec. S6. Technical details for proving the main results are in Sec. S7.

## S2. PRELIMINARIES

### A. Definitions and settings

We consider a one-dimensional system of  $n$  qudits, where the local dimension is  $d$ , and a quantum circuit with a fixed two-qudit gate  $u$  sandwiched by Haar random single qudit gates. We call such random two-qudit gates *u-structured random gates*. Formally, it is the probability distribution  $\mu_u$  in the unitary group  $U(d^2)$  defined by first choosing four Haar single qudit gate Haar randomly  $v_i$ , for  $i \in \{1, 2, 3, 4\}$ , and then applying them to  $u$  giving  $(v_1 \otimes v_2)u(v_3 \otimes v_4)$ , as illustrated in Fig. 1 (a). Such a gate set of  $u$ -structured random gates does not form a group in general, which is in contrast to well-studied gates such as two-qudit Haar or Clifford gates. A two-qudit unitary gate  $u$  acting on  $i$ - and  $j$ -th qudits is denoted by  $u_{i,j}$ .

For architecture of quantum circuits, we specifically consider the following: *u-structured local random circuit*, illustrated in Fig. 1 (a) in the main text, is a probability distribution  $\nu_u^L$  on  $U(d^n)$  defined by first randomly choosing a pair of adjacent qudits and then applying a structured random gate drawn from  $\nu_u$  on the qudits, and *u-structured brick-wall random circuit*  $\nu_u^B$ , illustrated in Fig. 1 (b), is defined by first applying  $\bigotimes_i w_{i,i+1}$  and then applying  $\bigotimes_i w_{i+1,i+2}$ , where each  $w$  is drawn from  $\mu_u$ . As for  $u$ -structured brick-wall circuits, we assume that the number of qudits  $n$  is even. For technical simplicity, we assume that both architectures satisfy periodic boundary conditions. Nevertheless, we expect that the technique we use for our proofs also works for the cases of open boundary conditions. For local and brick-wall random circuits consisting of Haar random two-qudit unitary gates, we call them local Haar random circuits and brick-wall Haar random circuits, denoted by  $\nu_H^L$  and  $\nu_H^B$ , respectively. A concatenation of two unitaries drawn from probability distributions  $\nu_1$  and  $\nu_2$  can be described by the convolution  $\nu_1 * \nu_2$ . Then, the probability distribution of a random circuit  $\nu$  with circuit depth  $t$  is described as the  $t$ -fold convolution  $\nu^{*t}$ , which we also denote by  $\nu_t$ . We note that, in the context of entanglement dynamics, an earlier work on random circuits [73] has also considered random circuits with certain gate structure, such as taking  $u$  as CNOT in the above  $u$ -structured random circuits. Also, in the reference, the second-moment operator of the Haar local random circuit is diagonalized by mapping it to free-fermionic systems. Here, we consider the general case of an arbitrary  $u$  and extend the mapping to structured random circuits under the solvable condition, which will be explained later, in order to investigate how the global randomness depends on  $u$ .

The key object of this work is the moment operator of random quantum circuits. The  $k$ -th moment operator  $M_\nu^{(k)}$  of a probability distribution  $\nu$  on the unitary group is defined by the operator acting on  $2k$  copies of physical systems,

$$M_\nu^{(k)} = \int U^{\otimes k,k} d\nu(U), \quad (\text{S1})$$

where for an operator  $A$ ,  $A^{\otimes k,k} = A^{\otimes k} \otimes \bar{A}^{\otimes k}$  and  $\bar{A}$  is the complex conjugate of  $A$ . The moment operators have the largest eigenvalue 1 and the corresponding eigenspace has dimension at least  $k!$  when  $k \leq d^n$ . We denote the moment operator  $M_\nu^{(k)}$  with  $\nu = \nu_u^a$ , for  $a = L, B$ , by  $M_{a,u}^{(k)}$ . Moreover, the  $n$ -qudit moment operator of the global Haar random ensemble, local Haar random circuits, and brick-wall Haar random circuits are denoted by  $M_H^{(k)}$ ,  $M_{L,H}^{(k)}$ , and  $M_{B,H}^{(k)}$ , respectively. For a probability distribution of random circuits  $\nu_t$  with depth  $t$ , the moment operator is a multiplication of  $t$  individual moment operators, that is

$$M_{\nu_t}^{(k)} = (M_\nu^{(k)})^t. \quad (\text{S2})$$

Note that  $(M_H^{(k)})^t = (M_H^{(k)})$  due to its invariance.

The convergence speed of random circuits to Haar random ensemble, in terms of  $k$ -th moment, is characterized by the spectrum of it. This is because we have  $(M_\nu^{(k)})^t = M_H^{(k)} + R$ , where  $R$  involves the factors  $\lambda_i^t$  for each eigenvalue  $\lambda_i$  of the moment

operator. We note that the eigenvalues of  $M_\nu^{(k)}$  can be complex numbers in general and the eigenvalues with maximum absolute value are 1. We write the eigenvalues of  $M_\nu^{(k)}$  in the non-increasing order in absolute value  $|\lambda_1| \geq |\lambda_2| \geq |\lambda_3| \geq \dots$ , where we have  $\lambda_i = 1$  for  $i = 1, 2, \dots, k!$ , when  $k \leq d^n$ . We then define *spectral gap*  $\Delta_\nu^{(k)}$  of a moment operator  $M_\nu^{(k)}$  by  $\Delta_\nu^{(k)} = 1 - |\lambda_{k!+1}|$ , which is the difference between the largest and second-largest eigenvalues in absolute value of the moment operator. When the moment operator  $M_\nu^{(k)}$  is Hermitian, the gap is equal to the distance between random circuits  $\nu$  and the global Haar random unitaries in the Schatten  $\infty$ -norm, namely  $\|M_\nu^{(k)} - M_H^{(k)}\|_\infty = 1 - \Delta_\nu^{(k)}$ . For a depth  $t$  random circuit  $\nu_t$ , when  $M_{\nu_t}^{(k)}$  is Hermitian, we have

$$\|M_{\nu_t}^{(k)} - M_H^{(k)}\|_\infty = \left(1 - \Delta_\nu^{(k)}\right)^t. \quad (\text{S3})$$

When  $M_{\nu_t}^{(k)}$  is non-Hermitian, which is the case for the brick-wall architecture, the equality between the distance and the spectral gap of  $M_{\nu_t}^{(k)}$  is not necessarily true. Still, they become asymptotically equal in depth  $t$  as follows. Since the largest eigenvalue in absolute value of  $M_{\nu_t}^{(k)} - M_H^{(k)}$  is  $1 - \Delta_\nu^{(k)}$ , we have  $\left(\|M_{\nu_t}^{(k)} - M_H^{(k)}\|_\infty\right)^{1/t} = 1 - \Delta_\nu^{(k)}$  in the large  $t$  limit, where this follows from the Gelfand formula [74]. It implies that  $\log_{1-\Delta_\nu^{(k)}} \|M_{\nu_t}^{(k)} - M_H^{(k)}\|_\infty = t + o(t)$ , and equivalently, we obtain

$$\|M_{\nu_t}^{(k)} - M_H^{(k)}\|_\infty = \left(1 - \Delta_\nu^{(k)}\right)^{t+o(t)}, \quad (\text{S4})$$

which includes Eq. (S3) as a special case. We note that, although we will focus on the value of  $\Delta_\nu^{(2)}$  in Sec. S4, we can also calculate  $\|M_{\nu_t}^{(2)} - M_H^{(2)}\|_\infty$  for small  $t$  by the method developed in this paper. Furthermore, the norm  $\|M_{\nu_t}^{(k)} - M_H^{(k)}\|_\infty$  upper-bounds the error and hence the required circuit depth to form approximate unitary  $k$ -designs [25, 28]. Here, exact and approximate unitary  $k$ -designs are unitary ensembles whose  $k$ -th moment operators are exactly and approximately equal to that of the global Haar random unitaries, respectively. Practically, many applications for quantum information processing employ the second-moment property, or unitary 2-designs [48, 49, 75], applying to computational advantage [9, 65, 66], quantum channel fidelity estimation [48], random coding [67, 68], and entanglement detection [69], and so on.

In this work, we focus on the second moment that corresponds to  $k = 2$ . The eigenspace  $V_1$  of the second-moment operators with eigenvalue 1 is spanned by the  $n$ -fold vectorization of the identity and SWAP gates acting on two copies of physical systems, namely

$$V_1 = \text{span} \left\{ |I\rangle^{\otimes n}, |S\rangle^{\otimes n} \right\}, \quad (\text{S5})$$

where  $n$  is the number of qudits. Here, for an operator  $A$  acting on  $\mathbb{C}^d \otimes \mathbb{C}^d$ , which is the space of two copies of qudit states, we define  $|A\rangle$  by the vectorization of  $A$ , that is  $|A\rangle = \sum_{i,j=1}^d (A \otimes I)(|i\rangle \otimes |j\rangle) \otimes (|i\rangle \otimes |j\rangle)$ . The vectorization of  $I$  and  $S$  are shown in Fig. S1 (a). We denote its orthogonal complement subspace by  $V_1^\perp$ . As in the main text, we define two notions of more randomness as follows, which is a restatement of Definitions 1 and 2.

**Definition S1** (More randomness). *Let  $\nu$  and  $\mu$  be probability distributions of random circuits. The distribution  $\nu$  is said to be more random with respect to spectral gaps than  $\mu$  if the inequality*

$$\Delta_\nu^{(2)} > \Delta_\mu^{(2)} \quad (\text{S6})$$

*holds. When  $M_\nu^{(2)}$  and  $M_\mu^{(2)}$  are Hermitian operators,  $\nu$  is said to be more random with respect to positivity than  $\mu$  if the restriction of the operator to  $V_1^\perp$ ,*

$$M = M_\mu^{(2)} \Big|_{V_1^\perp} - M_\nu^{(2)} \Big|_{V_1^\perp}, \quad (\text{S7})$$

*is a positive operator, i.e.,  $\langle \psi | (M_\mu^{(2)} - M_\nu^{(2)}) | \psi \rangle > 0$  for all  $|\psi\rangle \in V_1^\perp$ .*

As we explain in the main text, when the second-largest eigenvalue in absolute value is positive, the definition based on positivity is stronger than that based on gap, where this reduction follows from Weyl's monotonicity theorem [50]. In addition to it, we remark on the definition based on positivity and justify why it is a natural definition of more randomness. One particular feature of global Haar random unitaries is that an expectation value is highly concentrated at its mean value, highlighted by the concentration bound [51]. In this context, the bound on the second-moment implies the bound on the variance. Specifically, more randomness of  $\nu$  than  $\mu$  with respect to positivity implies that the probability distribution of  $|\langle \psi | U | \psi \rangle|^2$  drawn  $U$  from a structured random circuit  $\nu$ , for a state vector  $|\psi\rangle$ , is more concentrated at its mean value than that of another structured random circuit  $\mu$ , where it follows from the Chebyshev's inequality. This kind of concentration bound is used, for example, to prove the equilibration of the random product states [52] and lower-bound the circuit complexity of the random unitary ensemble [20, 43].

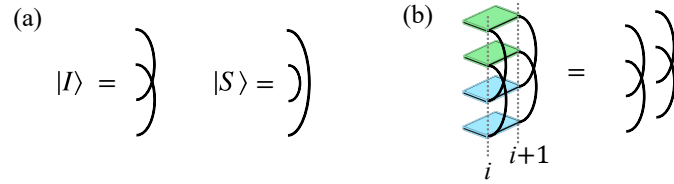


FIG. S1. Vectorization of the identity and SWAP gates. The identity and SWAP gates are graphically described (a), where each arc is the unnormalized Bell state vector  $\sum_{j=1}^d |j, j\rangle$ . The equality  $u_{i,i+1}^{\otimes 2,2} |I\rangle \otimes |I\rangle = |I\rangle \otimes |I\rangle$  is graphically described (b), where the green and blue boxes are  $u_{i,i+1}$  and  $\bar{u}_{i,i+1}$ , respectively, and  $i$  and  $i+1$  are the site indices of the qudits.

## B. Weingarten calculus

The moment operator  $M_{a,u}^{(2)}$ , for  $a = L, B$ , involves the second moment of the two-qudit gate  $u_{i,i+1}$  sandwiched by single-qudit Haar random gates, which is

$$W_{i,i+1}^u = \int ((v_3 \otimes v_4) u_{i,i+1} (v_1 \otimes v_2))^{\otimes 2,2} d\mu_{\text{H}}(v_1) d\mu_{\text{H}}(v_2) d\mu_{\text{H}}(v_3) d\mu_{\text{H}}(v_4), \quad (\text{S8})$$

where  $\mu_{\text{H}}$  is the Haar measure on  $U(d)$ . The moment operators which we consider are written as

$$M_{L,u}^{(2)} = \frac{1}{n} \sum_{i=1}^n W_{i,i+1}^u, \quad (\text{S9})$$

$$M_{B,u}^{(2)} = \bigotimes_{i=1}^{\frac{n}{2}} W_{2i,2i+1}^u \bigotimes_{i=1}^{\frac{n}{2}} W_{2i-1,2i}^u, \quad (\text{S10})$$

where we assume periodic boundary conditions  $W_{n,n+1}^u = W_{n,1}^u$  and  $n$  is an even number for the brick-wall architecture.

We can integrate single-qudit unitaries in Eq. (S8) by using the Weingarten calculus [76] as follows. Let  $S_2$  be the symmetric group of degree 2, and we consider the qudit representation, which is for example,  $S_2 = \{I, S\}$  with the two-qudit identity and the swap gate  $I$  and  $S$ , respectively. Because  $u^{\otimes 2,2} |I\rangle \otimes |I\rangle = |I\rangle \otimes |I\rangle$  (Fig. S1 (b)) and  $u^{\otimes 2,2} |S\rangle \otimes |S\rangle = |S\rangle \otimes |S\rangle$  for a two-qudit unitary gate  $u$ ,  $|I\rangle^{\otimes n}$  and  $|S\rangle^{\otimes n}$  are eigenvectors of  $M_{a,u}^{(2)}$  for  $a = L, B$  with eigenvalue 1, which is the largest eigenvalue for the moment operators. The Weingarten calculus then yields

$$\int v^{\otimes 2,2} d\mu_{\text{H}}(v) = \frac{1}{d^2 - 1} (|I\rangle \langle I| + |S\rangle \langle S| - \frac{1}{d} (|I\rangle \langle S| + |S\rangle \langle I|)), \quad (\text{S11})$$

and then Eq. (S8) becomes

$$W_{i,i+1}^u = \sum_{\sigma_1, \sigma_2, \sigma_3, \sigma_4 \in S_2} (|\tilde{\sigma}_3\rangle \langle \sigma_3| \otimes |\tilde{\sigma}_4\rangle \langle \sigma_4|) u_{i,i+1}^{\otimes 2,2} (|\tilde{\sigma}_1\rangle \langle \sigma_1| \otimes |\tilde{\sigma}_2\rangle \langle \sigma_2|), \quad (\text{S12})$$

where

$$\begin{aligned} |\tilde{I}\rangle &= \frac{1}{d^2 - 1} (|I\rangle - \frac{1}{d} |S\rangle), \\ |\tilde{S}\rangle &= \frac{1}{d^2 - 1} (|S\rangle - \frac{1}{d} |I\rangle). \end{aligned} \quad (\text{S13})$$

We note that the pair of the sets  $\{|I\rangle, |S\rangle\}$  and  $\{|\tilde{I}\rangle, |\tilde{S}\rangle\}$  is a biorthogonal system because they satisfy  $\langle \sigma | \tilde{\sigma} \rangle = 1$  and  $\langle \sigma | \tilde{\tau} \rangle = 0$  for  $\sigma \neq \tau$ . We define

$$W^u(\sigma_1 \sigma_2 \sigma_3 \sigma_4) = (\langle \sigma_3 | \otimes \langle \sigma_4 |) u^{\otimes 2,2} (|\tilde{\sigma}_1\rangle \otimes |\tilde{\sigma}_2\rangle), \quad (\text{S14})$$

or graphically, in a tensor-network language,

$$W^u(\sigma_1 \sigma_2 \sigma_3 \sigma_4) = \begin{array}{c} \textcircled{\tilde{\sigma}_1} \\ \textcircled{\tilde{\sigma}_2} \end{array} \begin{array}{c} \text{---} \\ \text{---} \\ \text{---} \\ \text{---} \end{array} \begin{array}{c} \text{---} \\ \text{---} \\ \text{---} \\ \text{---} \end{array} \begin{array}{c} \textcircled{\sigma_3} \\ \textcircled{\sigma_4} \end{array}, \quad (\text{S15})$$



where the box is 4-fold two-qudit gate  $u^{\otimes 2,2}$ . Then Eq. (S12) becomes,

$$\sum_{\sigma_1, \sigma_2, \sigma_3, \sigma_4 \in S_2} W^u(\sigma_1 \sigma_2 \sigma_3 \sigma_4) |\tilde{\sigma}_3\rangle \langle \sigma_1| \otimes |\tilde{\sigma}_4\rangle \langle \sigma_2|. \quad (\text{S16})$$

We also define the matrix  $\mathbf{W}^u$  by  $(\mathbf{W}^u)_{\sigma_1 \sigma_2, \tilde{\tau}_1 \tilde{\tau}_2} = \langle \sigma_1 \sigma_2 | W^u | \tilde{\tau}_1 \tilde{\tau}_2 \rangle$ .

### C. Matrix elements of moment operators

Here, we derive the matrix elements of the second-moment operator,  $W^u(\sigma_1 \sigma_2 \sigma_3 \sigma_4)$  for  $k = 2$ , which are

$$W^u(\sigma_1 \sigma_2 II) = \begin{cases} 1 & (\sigma_1 = \sigma_2 = I), \\ 0 & \text{otherwise,} \end{cases} \quad (\text{S17})$$

$$W^u(II \sigma_3 \sigma_4) = \frac{1}{(d^2 - 1)^2} \left( d^3 + d - \frac{\langle \sigma_3 | \otimes \langle \sigma_4 | u^{\otimes 2,2} | S \rangle \otimes | I \rangle}{d} - \frac{\langle \sigma_3 | \otimes \langle \sigma_4 | u^{\otimes 2,2} | I \rangle \otimes | S \rangle}{d} \right), \quad (\text{S18})$$

$$W^u(SI \sigma_3 \sigma_4) = \frac{1}{(d^2 - 1)^2} \left( -2d^2 + \langle \sigma_3 | \otimes \langle \sigma_4 | u^{\otimes 2,2} | S \rangle \otimes | I \rangle + \frac{\langle \sigma_3 | \otimes \langle \sigma_4 | u^{\otimes 2,2} | I \rangle \otimes | S \rangle}{d^2} \right), \quad (\text{S19})$$

for  $\sigma_3 \neq \sigma_4$ . Other weights are obtained by the spin-flip symmetry  $W(\sigma_1 \sigma_2 \sigma_3 \sigma_4) = W(\bar{\sigma}_1 \bar{\sigma}_2 \bar{\sigma}_3 \bar{\sigma}_4)$ , where  $\bar{I} = S$  and  $\bar{S} = I$ . We have

$$\begin{aligned} W^u(IIII) &= \frac{1}{(d^2 - 1)^2} \langle I | \otimes \langle I | u^{\otimes 2,2} | I \rangle \otimes | I \rangle + \frac{1}{d^2 (d^2 - 1)^2} \langle S | \otimes \langle S | u^{\otimes 2,2} | I \rangle \otimes | I \rangle \\ &\quad - \frac{1}{d (d^2 - 1)^2} \langle I | \otimes \langle S | u^{\otimes 2,2} | I \rangle \otimes | I \rangle - \frac{1}{d (d^2 - 1)^2} \langle S | \otimes \langle I | u^{\otimes 2,2} | I \rangle \otimes | I \rangle \\ &= \frac{d^4}{(d^2 - 1)^2} + \frac{d^2}{d^2 (d^2 - 1)^2} - \frac{2d^3}{d (d^2 - 1)^2} \\ &= 1, \end{aligned} \quad (\text{S20})$$

where we have used the equality  $u^{\otimes 2,2} | I \rangle \otimes | I \rangle = | I \rangle \otimes | I \rangle$ . Similarly, we obtain, for example,

$$\begin{aligned} W^u(ISII) &= \frac{1}{(d^2 - 1)^2} \langle I | \otimes \langle S | u^{\otimes 2,2} | I \rangle \otimes | I \rangle + \frac{1}{d^2 (d^2 - 1)^2} \langle S | \otimes \langle I | u^{\otimes 2,2} | I \rangle \otimes | I \rangle \\ &\quad - \frac{1}{d (d^2 - 1)^2} \langle I | \otimes \langle I | u^{\otimes 2,2} | I \rangle \otimes | I \rangle - \frac{1}{d (d^2 - 1)^2} \langle S | \otimes \langle S | u^{\otimes 2,2} | I \rangle \otimes | I \rangle \\ &= 0, \end{aligned} \quad (\text{S21})$$

$$\begin{aligned} W^u(IISI) &= \frac{1}{(d^2 - 1)^2} \langle I | \otimes \langle I | u^{\otimes 2,2} | S \rangle \otimes | I \rangle + \frac{1}{d^2 (d^2 - 1)^2} \langle S | \otimes \langle S | u^{\otimes 2,2} | S \rangle \otimes | I \rangle \\ &\quad - \frac{1}{d (d^2 - 1)^2} \langle I | \otimes \langle S | u^{\otimes 2,2} | S \rangle \otimes | I \rangle - \frac{1}{d (d^2 - 1)^2} \langle S | \otimes \langle I | u^{\otimes 2,2} | S \rangle \otimes | I \rangle \\ &= \frac{1}{(d^2 - 1)^2} \left( d^3 + d - \frac{\langle S | \otimes \langle I | u^{\otimes 2,2} | S \rangle \otimes | I \rangle}{d} - \frac{\langle S | \otimes \langle I | u^{\otimes 2,2} | I \rangle \otimes | S \rangle}{d} \right). \end{aligned} \quad (\text{S22})$$

### D. Qubit systems

Here, we derive the factors in the matrix elements of the second-moment operators in the case of a qubit system. For a two-qubit unitary gate  $u$ , we define its dual operator  $\tilde{u}$  by reshuffling the indices as

$$\langle i | \otimes \langle j | \tilde{u} | k \rangle \otimes | l \rangle = \langle i | \otimes \langle k | u | j \rangle \otimes | l \rangle. \quad (\text{S23})$$

With the parametrization  $u = e^{-i(\alpha XX + \beta YY + \gamma ZZ)}$ , we can write  $\langle I | \otimes \langle S | u^{\otimes 2,2} | I \rangle \otimes | S \rangle$  in terms of its dual operator as

$$\langle I | \otimes \langle S | u^{\otimes 2,2} | I \rangle \otimes | S \rangle = \text{Tr}(\tilde{u} \tilde{u}^\dagger \tilde{u} \tilde{u}^\dagger), \quad (\text{S24})$$

$$\tilde{u} = \begin{pmatrix} e^{-i\gamma} \cos(\alpha - \beta) & 0 & 0 & e^{i\gamma} \cos(\alpha + \beta) \\ 0 & -ie^{-i\gamma} \sin(\alpha - \beta) & -ie^{i\gamma} \sin(\alpha + \beta) & 0 \\ 0 & -ie^{i\gamma} \sin(\alpha + \beta) & -ie^{-i\gamma} \sin(\alpha - \beta) & 0 \\ e^{i\gamma} \cos(\alpha + \beta) & 0 & 0 & e^{-i\gamma} \cos(\alpha - \beta) \end{pmatrix}. \quad (\text{S25})$$

By straightforward calculation, we obtain

$$\langle I | \otimes \langle S | u^{\otimes 2,2} | I \rangle \otimes | S \rangle = 4(1 + \cos^2(2\alpha) \cos^2(2\beta) + \cos^2(2\beta) \cos^2(2\gamma) + \cos^2(2\gamma) \cos^2(2\alpha)). \quad (\text{S26})$$

We can compute  $\langle I | \otimes \langle S | u^{\otimes 2,2} | S \rangle \otimes | I \rangle$  by

$$\begin{aligned} \langle I | \otimes \langle S | u^{\otimes 2,2} | S \rangle \otimes | I \rangle &= \langle I | \otimes \langle S | u^{\otimes 2,2} \cdot \text{SWAP}^{\otimes 2,2} | I \rangle \otimes | S \rangle \\ &= 4(1 + \sin^2(2\alpha) \sin^2(2\beta) + \sin^2(2\beta) \sin^2(2\gamma) + \sin^2(2\gamma) \sin^2(2\alpha)), \end{aligned} \quad (\text{S27})$$

where we have used  $\text{SWAP} = e^{-\frac{\pi}{4}i(XX+YY+ZZ)}$  up to a phase factor.

### S3. PARAMETRIZATION OF MOMENT OPERATOR

#### A. Entangling power and gate typicality

Although a two-qudit gate can be characterized by  $d^2$  parameters in general, we find that the matrix element  $W^u(\sigma_1 \sigma_2 \sigma_3 \sigma_4)$  can be described by only two parameters. Here, we give a parametrization of the matrix element  $W^u(\sigma_1 \sigma_2 \sigma_3 \sigma_4)$  and hence the moment operators  $M_\nu^{(2)}$  for  $\nu = \nu_u^L, \nu_u^B$ , in terms of the entangling power  $e_u$  and the gate typically  $g_u$ , which are to be defined below. A meaningful notion of the *entangling power*  $e_u$  [53–56, 77] of a two-qudit unitary  $u$  is the entanglement

$$e_u = \frac{d+1}{d-1} \int E_l(u|\psi\rangle \otimes |\phi\rangle) d|\psi\rangle d|\phi\rangle \quad (\text{S28})$$

of random product states applied by  $u$ , where the integration is over the single-qudit Haar random state and  $E_l(|\Psi\rangle) = 1 - \text{Tr} \rho_A^2$ , with  $\rho_A = \text{Tr}_B |\Psi\rangle \langle \Psi|$ , is the linear entanglement entropy. Here,  $|\Psi\rangle$  is a state in a two-qudit system, where we define the subsystems  $A$  and  $B$  by the individual qudits. A similar entanglement measure of a unitary  $u$  is the operator entanglement entropy. Let  $|u\rangle$  be the normalized vectorization of a two-qudit unitary  $u$ , and we write the basis explicitly as  $|u\rangle = \frac{1}{d} (u_{A_1 B_1} \otimes I_{A_2 B_2}) \sum_{i,j=1}^d |i\rangle_{A_1} |j\rangle_{B_1} |i\rangle_{A_2} |j\rangle_{B_2}$ , and  $\rho_A(u) = \text{Tr}_{B_1 B_2} |u\rangle \langle u|$ . Then, the operator entanglement [78] of  $u$  is defined by

$$E(u) = 1 - \text{Tr} \rho_A(u)^2, \quad (\text{S29})$$

and this is equal to

$$E(u) = 1 - \frac{\langle I | \otimes \langle S | u^{\otimes 2,2} | I \rangle \otimes | S \rangle}{d^4}. \quad (\text{S30})$$

The entangling power of a two-qudit unitary  $u$  can be rewritten as

$$e_u = \frac{1}{E(\text{SWAP})} (E(u) + E(u \cdot \text{SWAP}) - E(\text{SWAP})), \quad (\text{S31})$$

where SWAP denotes the two-qudit swap gate. Throughout this work, we use SWAP for the two-qudit SWAP gate acting on one physical system and  $S$  for the swap operation acting on two copies of physical systems. For two-qubit gate  $u$ , the entangling power can take all the value within  $0 \leq e_u \leq \frac{2}{3}$ , where, for example, the CNOT gate and the iSWAP gate have  $e_u = \frac{2}{3}$ . For two-qudit gate  $u$  with local dimension  $d \geq 3$ , the value takes  $0 \leq e_u \leq 1$ . For Haar random two-qudit unitary gates, the averaged entangling power is

$$\begin{aligned} e_H &= \int e_u d\mu_H(u) \\ &= \frac{d^2 - 1}{d^2 + 1}. \end{aligned} \quad (\text{S32})$$

For example, in the case of qubit-system, we have  $e_H = \frac{3}{5}$ . In addition, the *gate typically*  $g_u$  [54–56], which is a complementary quantity to  $e_u$ , is defined by

$$g_u = \frac{1}{2E(\text{SWAP})} (E(u) - E(u \cdot \text{SWAP}) + E(\text{SWAP})). \quad (\text{S33})$$

For two-qudit gate  $u$  with local dimension  $d \geq 2$ , the value takes  $0 \leq g_u \leq 1$ , where  $g_u = 1$  and  $g_u = 0$  if  $u$  is the two-qudit SWAP gate and the identity gate, respectively. For Haar random two-qudit unitary gates, the averaged gate typicality is  $g_H = \int g_u d\mu_H(u) = \frac{1}{2}$ . We note that the second-moment operators of  $u$ -structured random circuits satisfying  $e_u = e_H$  and  $g_u = g_H$  are equal to those of Haar random circuits, because the second-moment operators only depend on  $e_u$  and  $g_u$  as we show in the next section.

We finally remark that there are limitations of feasible  $e_u$  and  $g_u$ , i.e., there does not necessarily exist a unitary gate  $u$  for  $e_u$  and  $g_u$  satisfying the conditions above. For a two-qubit unitary  $u$ , the values  $e_u$  and  $g_u$  are feasible if and only if they satisfy  $2g_u(1 - g_u) \leq e_u \leq 2g_u$ ,  $e_u \leq 2 - 2g_u$ , and  $e_u \leq \frac{2}{3}$  [55]. For a two-qutrit unitary, the constraint  $e_u \leq \frac{2}{3}$  is replaced by  $e_u \leq 1$ , and the range of  $e_u$  and  $g_u$  are numerically shown in Ref. [55], see the reference for more detail. In addition, the two-qudit unitary gates satisfying  $e_u = 2 - 2g_u$  are called dual-unitary gates [61–64], and those satisfying  $e_u = 1$  and  $g_u = \frac{1}{2}$  are called perfect tensors [79, 80].

## B. Moment operator and entanglement properties

We relate the matrix element of moment operators, the entangling power, and the gate typicality. By Eqs. (S31) and (S33), we have

$$E(u) = \frac{d^2 - 1}{2d^2} (e_u + 2g_u), \quad (\text{S34})$$

$$E(u \cdot \text{SWAP}) = \frac{d^2 - 1}{2d^2} (e_u - 2g_u + 2), \quad (\text{S35})$$

where we have used  $E(\text{SWAP}) = \frac{d^2 - 1}{d^2}$ . Then, we obtain by Eq. (S30),

$$\langle I | \otimes \langle S | u^{\otimes 2,2} | I \rangle \otimes | S \rangle = d^4 \left( 1 - \frac{d^2 - 1}{2d^2} (e_u + 2g_u) \right), \quad (\text{S36})$$

$$\langle I | \otimes \langle S | u^{\otimes 2,2} | S \rangle \otimes | I \rangle = d^4 \left( 1 - \frac{d^2 - 1}{2d^2} (e_u - 2g_u + 2) \right). \quad (\text{S37})$$

The matrix elements Eq. (S14) can be written in terms of  $e_u$  and  $g_u$  as

$$W^u(\sigma_1 \sigma_2 II) = \begin{cases} 1 & (\sigma_1 = \sigma_2 = I), \\ 0 & \text{otherwise,} \end{cases} \quad (\text{S38})$$

$$W^u(II SI) = \frac{de_u}{(d^2 + 1)e_H}, \quad (\text{S39})$$

$$W^u(IS IS) = 1 - \frac{e_u}{2e_H} - g_u, \quad (\text{S40})$$

$$W^u(ISSI) = -\frac{e_u}{2e_H} + g_u. \quad (\text{S41})$$

The other matrix elements are obtained by the spin-flip symmetry  $W(\sigma_1 \sigma_2 \sigma_3 \sigma_4) = W(\bar{\sigma}_1 \bar{\sigma}_2 \bar{\sigma}_3 \bar{\sigma}_4)$ , where  $\bar{I} = S$  and  $\bar{S} = I$ . For the derivation of the matrix elements, see Sec. S2C. When  $u$  is drawn from  $U(d^2)$  Haar randomly,

$$W^H(II SI) = \int W^u(II SI) d\mu_H(u) = \frac{d}{d^2 + 1} \quad (\text{S42})$$

and  $W^H(IS \sigma_3 \sigma_4) = \int W^u(II SI) d\mu_H(u) = 0$  for any  $\sigma_3, \sigma_4 \in \{I, S\}$ , which are consistent with the Boltzmann weights of Haar random gates that have been derived in Refs. [16, 81]. In order to diagonalize the moment operators of the structured random circuits, we assume that  $u$ -structured random gates satisfy the solvable condition  $W^u(ISSI) = 0$ , under which the operators are mapped to free-fermion chains. From Eq. (S41), the solvable condition is  $\frac{e_u}{2e_H} = g_u$ , or equivalently,

$$\frac{e_u}{g_u} = \frac{e_H}{g_H}, \quad (\text{S43})$$

## S4. MAIN RESULTS

Our main results are the exact spectrum and eigenvectors of the moment operators  $M_{a,u}^{(2)}$ , for  $a = L, B$  in the case of  $u$  satisfying the solvable condition  $W^u(ISSI) = 0$ . The result lead to more randomness of  $u$ -structured random circuits than random circuits consisting of two-qudit Haar random unitary gates, summarized in the following theorem.

**Theorem S1** (Restatement of Theorem 1 of the main text). *Let  $u$  be a two-qudit gate which satisfies the solvable condition  $W^u(ISSI) = 0$ . Then,  $u$ -structured local random circuits  $\nu_{L,u}$  and  $u$ -structured brick-wall random circuits  $\nu_{B,u}$  are more random with respect to the spectral gap than local Haar random circuits  $\nu_{\mathbb{H}}^L$  and brick-wall Haar random circuits  $\nu_{\mathbb{H}}^B$ , respectively, if and only if  $e_u > e_{\mathbb{H}}$ . Additionally, for a general two-qudit gate  $v$ ,  $\nu_v^L$  is more random with respect to positivity than  $\nu_{\mathbb{H}}^L$  if  $e_v > e_{\mathbb{H}}$  and  $g_v > g_{\mathbb{H}}$ .*

The proof of Theorem S1 is in Sec. S5 C, which follows from the diagonalization of moment operators stated in Theorem S2 and S4 which we show in the remainder of this section.

### A. Structured local random circuits

We prepare notations to state the rest of our results. We define the sets of labels that characterize the eigenstate: for even  $n$ ,

$$K_p := \left\{ \frac{2m-p}{n} \pi \mid m = -\frac{n}{2} + 1, -\frac{n}{2} + 2, \dots, \frac{n}{2} \right\}, \quad (\text{S44})$$

for  $p \in \{0, 1\}$ , and for odd  $n$ ,

$$K_p := \left\{ \frac{2m-p}{n} \pi \mid m = -\frac{n}{2} + \frac{1}{2}, -\frac{n}{2} + \frac{3}{2}, \dots, \frac{n}{2} - \frac{1}{2} \right\}, \quad (\text{S45})$$

We label the eigenvalues by  $p$  and  $i_p = \{i_{p,k}\}_{k \in K_p}$  with  $i_{p,k} \in \{0, 1\}$  satisfying  $\sum_{k \in K_p} i_{p,k} = 0 \pmod{2}$ . When it is clear that  $k$  is chosen from either  $K_0$  or  $K_1$ , we also express  $i_{p,k}$  using  $i_k$ . Additionally, we let

$$\eta_k = \frac{1}{2} \sum_{j=1}^n e^{ikj} X^{\otimes j-1} \otimes (Z - iY) \otimes I^{\otimes n-j}, \quad (\text{S46})$$

$$\eta_{1,k} = (\eta_k^\dagger \eta_{-k}), \quad (\text{S47})$$

$$\eta_{1,k}^\dagger = (\eta_k \eta_{-k}^\dagger)^\top, \quad (\text{S48})$$

$$\eta_{2,k} = (\eta_k^\dagger \eta_{-k} \eta_{k-\pi}^\dagger \eta_{\pi-k}), \quad (\text{S49})$$

$$\eta_{2,k}^\dagger = (\eta_k \eta_{-k}^\dagger \eta_{k-\pi} \eta_{\pi-k}^\dagger)^\top, \quad (\text{S50})$$

where  $X, Y$ , and  $Z$  are the Pauli matrices. We also define the change of basis matrix  $V$  from the computational basis  $\{|0\rangle, |1\rangle\}$  to  $\{|I\rangle, |S\rangle\}$  by  $V^\dagger |i_{\sigma_1}, i_{\sigma_2}, \dots, i_{\sigma_n}\rangle = |\sigma_1, \sigma_2, \dots, \sigma_n\rangle$ , where  $|i_I\rangle = |0\rangle$  and  $|i_S\rangle = |1\rangle$ . We obtain the diagonalization of the moment operator  $M_{L,u}^{(2)}$  that can be succinctly summarized in the following theorem.

**Theorem S2** (Diagonalization for structured local random circuits). *Let  $u$  be a two-qudit gate which satisfies  $W^u(ISSI) = 0$ . Then, the eigenvalues of  $M_{L,u}^{(2)}$  are obtained by*

$$\lambda_{p,i_p} = 1 - \frac{1}{n} \sum_{k \in K_p} \epsilon_k i_{p,k}, \quad (\text{S51})$$

where  $p \in \{0, 1\}$ ,  $\epsilon_k = \tilde{e}_u (1 - 2a_k)$ ,  $\tilde{e}_u = \frac{e_u}{e_{\mathbb{H}}}$ , and  $a_k = \frac{d}{d^2+1} \cos k$ . The corresponding left eigenvectors to  $\lambda_{0,i_0}$  and  $\lambda_{1,i_1}$  are, up to normalization factors,

$$\left( \langle 0|^{\otimes n} - \langle 1|^{\otimes n} \right) (\xi_0^\dagger)^{i_{0,0}} \prod_{k \in K_0 \setminus \{0\}} (\xi_k)^{i_{0,k}} V, \quad (\text{S52})$$

$$\left( \langle 0|^{\otimes n} + \langle 1|^{\otimes n} \right) \prod_{k \in K_1} (\xi_k)^{i_{1,k}} V, \quad (\text{S53})$$

respectively. Here, we have defined  $\xi_0 := \eta_0$ ,  $\xi_\pi := \eta_\pi$ , and for  $k \in K_0, K_1$  satisfying  $0 < k < \pi$ ,

$$\xi_{-k} := \boldsymbol{\eta}_{1,k} P_k \begin{pmatrix} 0 \\ 1 \end{pmatrix}, \quad (\text{S54})$$

$$\xi_k = (1 \ 0) P_k^{-1} \boldsymbol{\eta}_{1,k}^\dagger, \quad (\text{S55})$$

$$P_k = \begin{pmatrix} -z(1 - \cos k) & (1 + \cos k) \\ iz \sin k & iz \sin k \end{pmatrix}, \quad (\text{S56})$$

where  $z := \left(\frac{d+1}{d-1}\right)^2$ .

We add some remarks on Theorem S2. Since  $M_{L,u}^{(2)}$  is a Hermitian operator, the right eigenvectors of it are given by the complex conjugation of Eqs. (S53) and (S52). Moreover, when  $e_u > e_H$ , the  $i$ -th largest eigenvalues of  $M_{L,u}^{(2)}$  is less than the  $i$ -th largest eigenvalues of  $M_{L,H}^{(2)}$  for any  $i \geq 2$ . In the qubit case of  $d = 2$ , we have  $e_H = \frac{3}{5}$ , while  $u$ -structured random gates can take at most  $e_u = \frac{2}{3}$ .

As a corollary of Theorem S2, we obtain the spectral gap of the moment operator of structured local random circuits.

**Corollary S3** (Spectral gap of structured local random circuits). *Let  $u$  be a two-qudit gate which satisfies  $W^u(ISSI) = 0$ . The spectral gap of  $M_{L,u}^{(2)}$  is*

$$\frac{2e_u}{ne_H} \left(1 - \frac{2d}{d^2 + 1} \cos \frac{\pi}{n}\right). \quad (\text{S57})$$

## B. Structured brick-wall random circuits

Next, we state the result on the diagonalization of the moment operator of  $u$ -structured brick-wall random circuits.

**Theorem S4** (Diagonalization for structured brick-wall circuits). *Let  $u$  be a two-qudit gate which satisfies  $W^u(ISSI) = 0$ . Then, the eigenvalues of  $M_{B,u}^{(2)}$  are obtained by*

$$\lambda_{p,i_p} = \prod_{k \in K_p} (\lambda_k)^{i_k}, \quad (\text{S58})$$

where  $p \in \{0, 1\}$  and

$$\lambda_k = \left( a_k \tilde{e}_u + \sqrt{a_k^2 \tilde{e}_u^2 + 1 - \tilde{e}_u} \right)^2. \quad (\text{S59})$$

The corresponding left eigenvectors to  $\lambda_{0,i_0}$  and  $\lambda_{1,i_1}$  are, up to normalization factors,

$$\left( \langle 0|^{\otimes n} - \langle 1|^{\otimes n} \right) \prod_{-\pi < k < 0: k \in K_0} \left( \zeta_{R,k}^\dagger \right)^{i_{0,k}} \prod_{0 \leq k \leq \pi: k \in K_0} \left( \zeta_{L,k} \right)^{i_{0,k}} V, \quad (\text{S60})$$

$$\left( \langle 0|^{\otimes n} + \langle 1|^{\otimes n} \right) \prod_{-\pi < k < 0: k \in K_1} \left( \zeta_{R,k}^\dagger \right)^{i_{1,k}} \prod_{0 < k < \pi: k \in K_1} \left( \zeta_{L,k} \right)^{i_{1,k}} V, \quad (\text{S61})$$

respectively. Here, we have defined  $\zeta_l$  by, for  $0 < k < \frac{\pi}{2}$ ,

$$\left( \zeta_{L,k} \zeta_{L,\pi-k} \zeta_{L,k-\pi} \zeta_{L,k} \right) = \boldsymbol{\eta}_{2,k} W_k, \quad (\text{S62})$$

$$\left( \zeta_{R,k}^\dagger \zeta_{R,\pi-k}^\dagger \zeta_{R,k-\pi}^\dagger \zeta_{R,-k}^\dagger \right)^\top = W_k^{-1} \boldsymbol{\eta}_{2,k}^\dagger, \quad (\text{S63})$$

$$W_k = \begin{pmatrix} 1 & 1 & 1 & 1 \\ -iz \tan \frac{k}{2} & -iz \tan \frac{k}{2} & -i \cot \frac{k}{2} & -i \cot \frac{k}{2} \\ -ir_{2,k} \tan \frac{k}{2} & -ir_{1,k} \tan \frac{k}{2} & -ir_{1,k} \cot \frac{k}{2} & -ir_{2,k} \cot \frac{k}{2} \\ zr_{2,k} & zr_{1,k} & r_{1,k} & r_{2,k} \end{pmatrix}, \quad (\text{S64})$$

where  $z = \left(\frac{d+1}{d-1}\right)^2$  and  $r_{i,k} = \frac{\tilde{e}_u - 2 - (-1)^{i+2} \sqrt{a_k^2 \tilde{e}_u^2 + (1 - \tilde{e}_u)}}{\tilde{e}_u (1 + 2a_k)}$ , for  $i \in \{1, 2\}$ . Also,  $(\zeta_{L,0} \zeta_{L,\pi}) = \boldsymbol{\eta}_{1,0} W_0$ ,  $(\zeta_{R,0}^\dagger \zeta_{R,\pi}^\dagger)^\top = W_0^{-1} \boldsymbol{\eta}_{1,0}^\dagger$ ,  $(\zeta_{L,\frac{\pi}{2}} \zeta_{L,-\frac{\pi}{2}}) = \boldsymbol{\eta}_{1,\frac{\pi}{2}} W_{\frac{\pi}{2}}$ , and  $(\zeta_{R,\frac{\pi}{2}}^\dagger \zeta_{R,-\frac{\pi}{2}}^\dagger)^\top = W_{\frac{\pi}{2}}^{-1} \boldsymbol{\eta}_{1,\frac{\pi}{2}}^\dagger$ , where

$$W_0 = \begin{pmatrix} -r_{1,0} & -r_{2,0} \\ 1 & 1 \end{pmatrix}, \quad (\text{S65})$$

$$W_{\frac{\pi}{2}} = \begin{pmatrix} i & iz^{-1} \\ 1 & 1 \end{pmatrix}. \quad (\text{S66})$$

As a corollary, we obtain the spectral gap of the structured brick-wall circuits.

**Corollary S5** (Spectral gap of structured brick-wall random circuits). *Let  $u$  be a two-qudit gate which satisfies  $W^u(\text{ISSI}) = 0$ . The spectral gap of  $M_{B,u}^{(2)}$  is given by*

$$1 - \max\left(|\lambda_{\frac{\pi}{n}}|^2, \lambda_0 |\lambda_{\frac{2\pi}{n}}|\right), \quad (\text{S67})$$

where  $\lambda_k$  is defined in Eq. (S59). Moreover, when  $\lambda_{\frac{2\pi}{n}}$  is a real number, we have

$$\max\left(|\lambda_{\frac{\pi}{n}}|^2, \lambda_0 |\lambda_{\frac{2\pi}{n}}|\right) = \left(\lambda_{\frac{\pi}{n}}\right)^2, \quad (\text{S68})$$

and when  $\lambda_{\frac{\pi}{n}}$  is not a real number, we have

$$\max\left(|\lambda_{\frac{\pi}{n}}|^2, \lambda_0 |\lambda_{\frac{2\pi}{n}}|\right) = \lambda_0 \left(\frac{e_u}{e_H} - 1\right). \quad (\text{S69})$$

In the case of qubit system with  $n \geq 6$ , it is easy to check that  $\lambda_{\frac{2\pi}{n}}$  is always real and  $\max\left(|\lambda_{\frac{\pi}{n}}|^2, \lambda_0 |\lambda_{\frac{2\pi}{n}}|\right) = \left(\lambda_{\frac{\pi}{n}}\right)^2$  for arbitrary  $0 \leq e_u \leq \frac{2}{3}$ . We remark that if  $\lambda_k$  is real, it monotonically decreases in  $e_u$ . However, in general, we find that the spectral gap does not increase in  $e_u$ . For example, in the case of qutrit system ( $d=3$ ) with  $n = 6$ , we find by straightforward calculation that the gap Eq. (S67) decreases in increasing  $e_u$  at  $e_u = 0.86$ .

## S5. DIAGONALIZATION OF SECOND-MOMENT OPERATORS

### A. Local random circuits

In this section, we map the second-moment operators of structured local random circuits to free-fermion chains and show the more randomness with respect to the positivity. We then diagonalize them and give proof of Theorem S2. The derivations of Theorem S2 and Theorem S4 go similarly, while the former is much simpler, and we can regard the proof in this section as a warm-up for the latter.

#### 1. More randomness with respect to positivity

We consider the matrix representation of the second-moment operator  $M_{L,u}^{(2)}$  based on the biorthogonal basis defined just below of Eq. (S13). We first expand the operator by the orthogonal system as

$$M_{L,u}^{(2)} = \sum_{\sigma_1, \dots, \sigma_n, \tau_1, \dots, \tau_n} \left\langle \sigma_1, \sigma_2, \dots, \sigma_n \left| M_{L,u}^{(2)} \right| \tilde{\tau}_1, \tilde{\tau}_2, \dots, \tilde{\tau}_n \right\rangle |\tilde{\sigma}_1, \tilde{\sigma}_2, \dots, \tilde{\sigma}_n\rangle \langle \tau_1, \tau_2, \dots, \tau_n|, \quad (\text{S70})$$

We change the orthogonal system to the computational basis  $\{|i_{\sigma_1}, i_{\sigma_2}, \dots, i_{\sigma_n}\}_{i_{\sigma_1}, i_{\sigma_2}, \dots, i_{\sigma_n} \in \{0,1\}}$ , where  $|i_\sigma\rangle = |0\rangle$  for  $\sigma = I$  and  $|i_\sigma\rangle = |1\rangle$  for  $\sigma = S$ , and we define the operator as

$$M_{L,u} = \sum_{\sigma_1, \dots, \sigma_n, \tau_1, \dots, \tau_n} \left\langle \sigma_1, \sigma_2, \dots, \sigma_n \left| M_{L,u}^{(2)} \right| \tilde{\tau}_1, \tilde{\tau}_2, \dots, \tilde{\tau}_n \right\rangle |i_{\sigma_1}, i_{\sigma_2}, \dots, i_{\sigma_n}\rangle \langle i_{\tau_1}, i_{\tau_2}, \dots, i_{\tau_n}|. \quad (\text{S71})$$

We note that these operators are related by the similar transformation  $VM_{L,u}^{(2)}V^{-1} = M_{L,u}$ , where  $V$  is defined by  $V^\dagger|i_{\sigma_1}, i_{\sigma_2}, \dots, i_{\sigma_n}\rangle = |\sigma_1, \sigma_2, \dots, \sigma_n\rangle$ . By the representation of the matrix on the computational basis,  $M_{L,u}$  is written as

$$M_{L,u} = I - \frac{1}{n}H, \quad (\text{S72})$$

$$H = \sum_{i=1}^n A_{i,i+1}, \quad (\text{S73})$$

where  $A$  has the matrix form

$$A = - \begin{pmatrix} 0 & 0 & 0 & 0 \\ a & b & c & a \\ a & c & b & a \\ 0 & 0 & 0 & 0 \end{pmatrix}, \quad (\text{S74})$$

$$a = \frac{d}{d^2 + 1} \frac{e_u}{e_H}, \quad (\text{S75})$$

$$b = -\frac{e_u}{2e_H} - g_u, \quad (\text{S76})$$

$$c = -\frac{e_u}{2e_H} + g_u. \quad (\text{S77})$$

We call the operator  $H$  the *moment Hamiltonian*. We first consider the solvable case of  $c = 0$ , where the second-moment operator can be mapped to a free-fermion chain. The matrix  $A$  can be expanded by the Pauli operators as

$$A = -b \frac{I \otimes I - Z \otimes Z}{2} - a(I \otimes X + X \otimes I) \frac{I \otimes I + Z \otimes Z}{2} - \frac{c}{2}(X \otimes X + Y \otimes Y). \quad (\text{S78})$$

By rewriting it in terms of  $e_u$  and  $g_u$  under the solvable condition  $c = 0$ , we obtain

$$A = \frac{e_u}{e_H} \left( \frac{I \otimes I - Z \otimes Z}{2} - \frac{d}{d^2 + 1} (I \otimes X + X \otimes I) \frac{I \otimes I + Z \otimes Z}{2} \right). \quad (\text{S79})$$

It is proportional to  $\frac{e_u}{e_H}$  and therefore, from Eq. (S73), the moment Hamiltonian  $H$  is also proportional to it. This implies that the eigenvalues of  $H$  monotonically increase in  $e_u$ , and the eigenvectors do not depend on  $e_u$ . Thus, we have, when  $e_u > e_H$ ,

$$M_{L,u}^{(2)} \Big|_{V_1^\perp} < M_{L,H}^{(2)} \Big|_{V_1^\perp}, \quad (\text{S80})$$

where we have used the fact that  $V_1 = \text{span}\{|I\rangle^{\otimes n}, |S\rangle^{\otimes n}\}$  is the eigenspace of  $H$  with eigenvalue 0.

Next, we analyze  $M_{L,u}^{(2)}$  for general  $e_u$  and  $g_u$  without the solvable condition. We use the matrix representation of the moment operator in the orthonormal basis, introduced in Ref. [82],

$$|+\rangle = \frac{1}{\sqrt{2d(d+1)}}(|I\rangle + |S\rangle), \quad (\text{S81})$$

$$|-\rangle = \frac{1}{\sqrt{2d(d-1)}}(|I\rangle - |S\rangle). \quad (\text{S82})$$

We define the matrix form by, for  $l_k, m_k \in \{|+\rangle, |-\rangle\}$ ,

$$\left( M_{L,u}^{(+,-)} \right)_{l_1, l_2, \dots, l_n, m_1, m_2, \dots, m_n} = \left\langle l_1, l_2, \dots, l_n \Big| M_{L,u}^{(2)} \Big| m_1, m_2, \dots, m_n \right\rangle. \quad (\text{S83})$$

The biorthogonal system  $\{|I\rangle, |S\rangle\}, \{|\tilde{I}\rangle, |\tilde{S}\rangle\}$  and the orthogonal basis  $\{|+\rangle, |-\rangle\}$  are related by the matrix  $W$  [82],

$$W = \frac{1}{\sqrt{2d}} \begin{pmatrix} \frac{1}{\sqrt{d+1}} & \frac{1}{\sqrt{d+1}} \\ \frac{1}{\sqrt{d+1}} & \frac{1}{\sqrt{d+1}} \end{pmatrix}, \quad (\text{S84})$$

and we have the relationship between Eq. (S72) and Eq. (S83) as  $M_{L,u}^{(+,-)} = W^{\otimes n} M_{L,u} (W^{-1})^{\otimes n}$ . We then obtain

$$M_{L,u}^{(+,-)} = I - \frac{1}{n} H^{(+,-)}, \quad (\text{S85})$$

$$H^{(+,-)} = \sum_{i=1}^n A_{i,i+1}^{(+,-)}, \quad (\text{S86})$$

where  $A^{(+,-)}$  has the matrix form

$$A^{(+,-)} = \begin{pmatrix} \frac{e_u(d-1)}{2(d+1)} & 0 & 0 & -\frac{e_u}{2} \\ 0 & g_u & -g_u & 0 \\ 0 & -g_u & g_u & 0 \\ -\frac{e_u}{2} & 0 & 0 & \frac{e_u(d+1)}{2(d-1)} \end{pmatrix} \quad (\text{S87})$$

$$= e_u \begin{pmatrix} \frac{d-1}{2(d+1)} & 0 & 0 & -\frac{1}{2} \\ 0 & 0 & 0 & 0 \\ 0 & 0 & 0 & 0 \\ -\frac{1}{2} & 0 & 0 & \frac{d+1}{2(d-1)} \end{pmatrix} + g_u \begin{pmatrix} 0 & 0 & 0 & 0 \\ 0 & 1 & -1 & 0 \\ 0 & -1 & 1 & 0 \\ 0 & 0 & 0 & 0 \end{pmatrix}. \quad (\text{S88})$$

We find that the first and the second matrix in Eq. (S88), whose coefficients are  $e_u$  and  $g_u$ , respectively, are positive semi-definite matrices. Therefore, the second-moment operator  $M_{L,u}^{(2)}$  monotonically decreases in  $e_u$  and  $g_u$ , in the sense that  $M_{L,u}^{(2)}(e_u + e', g_u) \leq M_{L,u}^{(2)}(e_u, g_u)$  and  $M_{L,u}^{(2)}(e_u, g_u + g') \leq M_{L,u}^{(2)}(e_u, g_u)$  for  $e', g' \geq 0$ , where we explicitly described that  $M_{L,u}^{(2)}$  is a function of  $e_u$  and  $g_u$ . By combining these inequalities with Eq. (S80), we have  $M_{L,u}^{(2)}|_{V_1^\perp} < M_{L,H}^{(2)}|_{V_1^\perp}$  if  $e_u > e_H$  and  $g_u > g_H$ . This derivation of the operator inequality is independent of the architecture of local random circuits, and therefore the operator inequality holds for structured local random circuits on arbitrary spatial dimensions. We remark that the moment Hamiltonian  $H^{(+,-)}$  corresponds to a frustration-free  $XYZ$  chain in a magnetic field [83, 84].

## 2. Proof for Theorem S2

Under the solvable condition  $c = 0$ , we map the Pauli strings in Eq. (S78) to quadratic fermionic operators by the Jordan-Wigner transformation

$$c_j^\dagger = \frac{1}{2} X^{\otimes j-1} \otimes (Z + iY) \otimes I^{\otimes n-j}, \quad (\text{S89})$$

which imply

$$A_{1,2} = -\frac{b+2a}{2} + a(c_1^\dagger c_1 + c_2^\dagger c_2) + \frac{b}{2}(c_1^\dagger c_2 + c_2^\dagger c_1) + \frac{1}{2}(b+2a)c_1^\dagger c_2^\dagger + \frac{1}{2}(b-2a)c_2 c_1. \quad (\text{S90})$$

The moment Hamiltonian becomes

$$H = -\frac{b+2a}{2}n + \sum_{i=1}^{n-1} \left( a(c_i^\dagger c_i + c_{i+1}^\dagger c_{i+1}) + \frac{b}{2}(c_i^\dagger c_{i+1} + c_{i+1}^\dagger c_i) + \frac{b+2a}{2}c_i^\dagger c_{i+1}^\dagger + \frac{b-2a}{2}c_{i+1} c_i \right) \\ - (-1)^N \left( a(c_1^\dagger c_1 + c_n^\dagger c_n) + \frac{b}{2}(c_{n+1}^\dagger c_1 + c_1^\dagger c_{n+1}) + \frac{b+2a}{2}c_{n+1}^\dagger c_1^\dagger + \frac{b-2a}{2}c_1 c_{n+1} \right), \quad (\text{S91})$$

where  $N$  is the fermionic number operator defined as

$$N := \sum_{j=1}^n c_j^\dagger c_j. \quad (\text{S92})$$

Because  $(-1)^N$  commutes with the transfer matrix, we consider two subspaces with even and odd fermion number separately. We impose the anti-periodic boundary condition

$$c_{n+1} = -c_1, \quad (\text{S93})$$



if  $H$  acts on the even parity subspace, and periodic boundary conditions

$$c_{n+1} = c_1, \quad (\text{S94})$$

if  $H$  acts on the odd parity subspace.

Because of the translation symmetry of the moment Hamiltonian, we use the standard technique of the discrete Fourier-transform of the fermionic operators: for  $j = 1, 2, \dots, n$ ,

$$c_j^\dagger = \frac{1}{\sqrt{n}} \sum_k e^{ikj} \eta_k^\dagger, \quad (\text{S95})$$

where  $k$  is summed over  $K_0$ , defined in Eqs. (S44) and (S45), when  $H$  acts on the odd parity subspace, and it is summed over  $K_1$  when  $H$  acts on the even parity subspace. The sets  $K_p$ , for  $p \in \{0, 1\}$ , were chosen so that the annihilation operators Eq. (S95) obey the boundary conditions in Eqs. (S93) and (S94). Conversely, we have, by the inverse Fourier transformation,

$$\eta_k^\dagger = \frac{1}{\sqrt{n}} \sum_{j=1}^n e^{-ikj} c_j^\dagger. \quad (\text{S96})$$

Then, the moment Hamiltonian becomes

$$H = -\frac{b+2a}{2}nI + (H^0 \oplus H^1), \quad (\text{S97})$$

$$H^p = \sum_{0 < k < \pi: k \in K_p} H_k + \delta_p(b+2a)\eta_0^\dagger\eta_0 - \delta_{p,n}(b-2a)\eta_\pi^\dagger\eta_\pi, \quad (\text{S98})$$

$$H_k = (2a + b \cos k)(\eta_k^\dagger\eta_k + \eta_{-k}^\dagger\eta_{-k}) - i(b+2a) \sin k \eta_k^\dagger\eta_{-k}^\dagger + i(b-2a) \sin k \eta_{-k}\eta_k, \quad (\text{S99})$$

where  $\delta_p = 1 - p$ ,  $\delta_{p,n} = \frac{1+(-1)^{p+n}}{2}$ , for  $p \in \{0, 1\}$ . We can put the matrices  $H_k$  in the diagonal form as

$$\begin{aligned} H_k &= 2a + b \cos k + \begin{pmatrix} \eta_k^\dagger & \eta_{-k} \end{pmatrix} \begin{pmatrix} 2a + b \cos k & -i \sin k(b+2a) \\ i \sin k(b-2a) & -2a - b \cos k \end{pmatrix} \begin{pmatrix} \eta_k \\ \eta_{-k}^\dagger \end{pmatrix} \\ &= 2a + b \cos k + \begin{pmatrix} \xi_{\text{R},k}^\dagger & \xi_{\text{L},-k} \end{pmatrix} \begin{pmatrix} \epsilon_k & 0 \\ 0 & -\epsilon_k \end{pmatrix} \begin{pmatrix} \xi_{\text{L},k} \\ \xi_{\text{R},-k}^\dagger \end{pmatrix}, \end{aligned} \quad (\text{S100})$$

where

$$\epsilon_k = -b - 2a \cos k, \quad (\text{S101})$$

and the right (left) fermionic eigenmodes  $\xi_{\text{R},pk}$  ( $\xi_{\text{L},pk}$ ) are given by, for  $0 < k < \pi$ ,

$$\begin{pmatrix} \xi_{\text{R},k}^\dagger & \xi_{\text{L},-k} \end{pmatrix} = \begin{pmatrix} \eta_k^\dagger & \eta_{-k} \end{pmatrix} P_k, \quad (\text{S102})$$

$$\begin{pmatrix} \xi_{\text{L},k} \\ \xi_{\text{R},-k}^\dagger \end{pmatrix} = P_k^{-1} \begin{pmatrix} \eta_k \\ \eta_{-k}^\dagger \end{pmatrix}, \quad (\text{S103})$$

with the diagonalizing matrix  $P_k$  of the matrix in the right-hand side in Eq. (S100), that is,

$$P_k = \begin{pmatrix} -(b-2a)(1-\cos k) & (b+2a)(1+\cos k) \\ i \sin k(b-2a) & i \sin k(b-2a) \end{pmatrix}. \quad (\text{S104})$$

From Eqs. (S75), (S76), the diagonalizing matrix can be rewritten as

$$P_k = \begin{pmatrix} -z(1-\cos k) & 1+\cos k \\ iz \sin k & iz \sin k \end{pmatrix}, \quad (\text{S105})$$

where  $z := \left(\frac{d+1}{d-1}\right)^2$  and we omit the scalar factor, which is irrelevant to the diagonalization. We note that the diagonalizing matrix  $P_k$  is always invertible because it is full rank for  $d \geq 2$ , and the inverse of Eq. (S105) is

$$P_k^{-1} = \frac{1}{1+z+(1-z)\cos k} \begin{pmatrix} -1 & -\frac{i(\cos k+1)}{z \sin k} \\ 1 & i \frac{(\cos k-1)}{\sin k} \end{pmatrix}. \quad (\text{S106})$$

Because  $H_k$  is a non-Hermitian matrix, we have  $\xi_{R,k} \neq \xi_{L,k}$ . Still, the right and left fermionic modes satisfy the fermionic commutation relations

$$\{\xi_{R,k}^\dagger, \xi_{L,l}\} = \delta_{k,l}, \quad (\text{S107})$$

$$\{\xi_{M,k}^\dagger, \xi_{M,l}\} = 0, \text{ for } M = R, L. \quad (\text{S108})$$

These relations imply that

$$H_k = 2a + b \cos k + \epsilon_k (\xi_{R,k}^\dagger \xi_{L,k} + \xi_{R,-k}^\dagger \xi_{L,-k} - 1). \quad (\text{S109})$$

In addition, we define  $\xi_{R,l}$  and  $\xi_{L,l}$  by  $\eta_l$  for  $l = 0, \pi$ .

Let  $\langle \text{vac} |_{\xi,1}$  be the left vacuum in the even parity subspace, which satisfies

$$\langle \text{vac} |_{\xi,1} \xi_{R,k}^\dagger = 0, \text{ for } \forall k \in K_1. \quad (\text{S110})$$

From Eqs. (S97), (S98), and (S109), the eigenvalues  $\lambda_{1,i_1}$  and corresponding left eigenvectors  $\langle i |_{\xi,1}$  of  $H$  restricted to the even parity subspace are

$$\lambda_{1,i_1} = -\frac{b+2a}{2}n + \sum_{0 < k < \pi: k \in K_1} (2a + b \cos k + \epsilon_k (i_k + i_{-k} - 1)) + \delta_{1,n} \epsilon_\pi i_\pi, \quad (\text{S111})$$

$$\langle i |_{\xi,1} = \langle \text{vac} |_{\xi,1} \prod_{k \in K_1} (\xi_{L,k})^{i_k}, \quad (\text{S112})$$

where in the even parity subspace,  $\delta_n = 1$  or  $\delta_n = 0$  for odd  $n$  or even  $n$ , respectively, we have defined  $i_1 = \{i_k\}_{k \in K_1}$ , with  $i_k \in \{0, 1\}$  for each  $k \in K_1$ , and the number of eigenmodes is restricted to be even number, namely,

$$\sum_{k \in K_1} i_k = 0 \pmod{2}. \quad (\text{S113})$$

Because  $\sum_{k \in K_1} \cos k = 0$  and  $\pi \in K_1$  only if  $n$  is odd, we have  $\sum_{0 < k < \pi: k \in K_1} \cos k = \delta_{1,n}/2$ , and we can compute Eq. (S111) furthermore as

$$\begin{aligned} \lambda_{1,i_1} &= -\frac{b+2a}{2}n + 2a \left\lfloor \frac{n}{2} \right\rfloor + b \frac{\delta_{1,n}}{2} + \sum_{0 < k < \pi: k \in K_1} \epsilon_k (i_k + i_{-k} - 1) + \delta_{1,n} \epsilon_\pi i_\pi \\ &= -\frac{b+2a}{2}n + 2a \left\lfloor \frac{n}{2} \right\rfloor + b \frac{\delta_{1,n}}{2} + \sum_{0 < k < \pi: k \in K_1} \epsilon_k (i_k + i_{-k}) + b \left\lfloor \frac{n}{2} \right\rfloor + a \delta_{1,n} + \delta_{1,n} \epsilon_\pi i_\pi \\ &= \sum_{0 < k < \pi: k \in K_1} \epsilon_k (i_k + i_{-k}) + \delta_{1,n} \epsilon_\pi i_\pi. \end{aligned} \quad (\text{S114})$$

By Eqs. (S32), (S75), (S76), and (S101), we have

$$\begin{aligned} \epsilon_k &= e_u \left( \frac{d^2 + 1}{d^2 - 1} - \frac{2d}{d^2 - 1} \cos k \right) \\ &= \frac{e_u}{e_H} \left( 1 - \frac{2d}{d^2 + 1} \cos k \right). \end{aligned} \quad (\text{S115})$$

and it is positive for an arbitrary integer  $d \geq 2$  and an arbitrary number  $0 \leq e_u \leq 1$ . Therefore, by Eq. (S114), the minimum eigenvalue of  $H$  in the even parity subspace is 0 and the corresponding left eigenvector is the vacuum  $\langle \text{vac} |_{\xi,1}$ .

Likewise, let  $\langle \text{vac} |_{\xi,0}$  be the left vacuum in the odd parity subspace, which satisfies

$$\langle \text{vac} |_{\xi,0} \xi_{R,k}^\dagger = 0, \text{ for } \forall k \in K_0. \quad (\text{S116})$$

We find the eigenvalues and corresponding left eigenvectors of  $H$  in the odd parity subspace, which are

$$\lambda_{0,i_0} = -\frac{b+2a}{2}n + \sum_{0 < k < \pi: k \in K_0} (2a + b \cos k + \epsilon_k (i_k + i_{-k} - 1)) - \epsilon_0 i_0 + \delta_{0,n} \epsilon_\pi i_\pi \quad (\text{S117})$$

$$= \sum_{0 < k < \pi: k \in K_0} \epsilon_k (i_k + i_{-k}) + (1 - i_0) \epsilon_0 + \delta_{0,n} \epsilon_\pi i_\pi,$$

$$\langle i |_{\xi,0} = \langle \text{vac} |_{\xi,0} \prod_{k \in K_0} (\xi_{L,k})^{i_k}, \quad (\text{S118})$$

where in the odd parity subspace,  $\delta_{0,n} = 0$  ( $\delta_{0,n} = 1$ ) for odd  $n$  (even  $n$ ), and we have defined  $\mathbf{i}_0 = \{i_k\}_{k \in K_0}$ , with  $i_k \in \{0, 1\}$  for each  $k \in K_0$ , and the number of the eigenmodes is odd, namely,

$$\sum_{k \in K_0} i_k = 1 \pmod{2}. \quad (\text{S119})$$

We note that in the statement of Theorem S2, we flip the value  $i_0 \in \mathbf{i}_0$  by changing it into  $i_0 + 1 \pmod{2}$  and the condition becomes  $\sum_{k \in K_0} i_k = 0 \pmod{2}$ , so that  $\mathbf{i}_0 = \{0\}^{\times |K_0|}$  implies an eigenvector with eigenvalue 1.

Because  $\epsilon_k$  is positive, the lowest eigenvalue of  $H$  restricted to the odd parity subspace is 0 and the corresponding left eigenvector is

$$\langle \text{vac} |_{\xi,0} \xi_{L,0}. \quad (\text{S120})$$

Finally, we translate the results above into the eigenvalues and eigenvectors of the moment operator  $M_{L,u}^{(2)}$ . From Eqs. (S72), the eigenvalues of  $M_{L,u}^{(2)}$  are given by

$$1 - \frac{\lambda_{p,i_p}}{n}. \quad (\text{S121})$$

The corresponding left eigenvectors are given by Eqs. (S112) and (S118). Because the entangling power of a unitary  $u$  is the same as that of  $u^\dagger$ , namely  $e_u = e_{u^\dagger}$ ,  $M_{L,u}^{(2)}$  is a Hermitian operator, and its right eigenvectors are given by the conjugate transpose of the left eigenvectors. We give a more explicit formula for the eigenvectors as the followings. Since  $\langle I |^{\otimes n}$  and  $\langle S |^{\otimes n}$  are the left eigenvectors of  $M_{L,u}^{(2)}$  with eigenvalue 1, the left eigenvectors of  $H$  with eigenvalue 0 must be in the form:

$$\langle \text{vac} |_{\xi,1} = p_1 \langle 0 |^{\otimes n} + p_2 \langle 1 |^{\otimes n}, \quad (\text{S122})$$

$$\langle \text{vac} |_{\xi,0} \xi_{L,0} = q_1 \langle 0 |^{\otimes n} + q_2 \langle 1 |^{\otimes n}, \quad (\text{S123})$$

for some constant numbers  $p_i$  and  $q_i$  for  $i \in \{0, 1\}$ . From the condition of being vacuum Eq. (S110) with the definition of  $\xi_{R,k}$  Eq. (S102), we need to find  $p_1$  and  $p_2$  such that

$$\left( p_1 \langle 0 |^{\otimes n} + p_2 \langle 1 |^{\otimes n} \right) \left( (1 - \cos k) \eta_k^\dagger - i \sin k \eta_{-k} \right) = 0, \text{ for } \forall k \in K_1. \quad (\text{S124})$$

From the relationship  $\eta_k^\dagger = \frac{1}{\sqrt{n}} \sum_{j=1}^n e^{-ikj} c_j^\dagger$ , the left-hand side of Eq. (S124) becomes, up to a constant factor,

$$\begin{aligned} & \left( p_1 \langle 0 |^{\otimes n} + p_2 \langle 1 |^{\otimes n} \right) \sum_{j=1}^n e^{-ikj} \left( (1 - \cos k) c_j^\dagger - i \sin k c_j \right) \\ &= \frac{1}{2} \left( p_1 \langle 0 |^{\otimes n} + p_2 \langle 1 |^{\otimes n} \right) \sum_{j=1}^n e^{-ikj} X^{\otimes j-1} \otimes \left( (1 - e^{ik})Z + i(1 - e^{-ik})Y \right) \otimes I^{\otimes n-j}, \\ &= \frac{1}{2} \sum_{j=1}^n e^{-ikj} \left[ p_1 \langle 1 |^{\otimes j-1} \otimes \left( \langle 0 | (1 - e^{ik}) + \langle S | (1 - e^{-ik}) \right) \otimes \langle I |^{\otimes n-j} \right. \\ & \quad \left. - p_2 \langle 0 |^{\otimes j-1} \otimes \left( \langle 1 | (1 - e^{ik}) + \langle 0 | (1 - e^{-ik}) \right) \otimes \langle 1 |^{\otimes n-j} \right] \\ &= \frac{1}{2} \left( p_1 \langle 0 |^{\otimes n} (e^{-ik} - 1) + p_1 \langle 1 |^{\otimes n} e^{-ikn} (1 - e^{-ik}) + p_2 \langle 1 |^{\otimes n} (1 - e^{-ik}) + p_2 \langle 0 |^{\otimes n} e^{-ikn} (e^{-ik} - 1) \right) \\ &= \frac{1}{2} (e^{-ik} - 1) (p_1 - p_2) \left( \langle 0 |^{\otimes n} + \langle 1 |^{\otimes n} \right), \end{aligned} \quad (\text{S125})$$

where in the last equality, we have used  $e^{-ikn} = -1$  for  $k \in K_1$ . Therefore, from Eqs. (S124) and (S125), we have  $p_1 = p_2$ . Similarly, we find  $q_1 = -q_2$ , in the case of the odd subspace. By the normalization of the vacuum states with the equalities  $\langle I | I \rangle = \langle S | S \rangle = d^2$  and  $\langle I | S \rangle = d$ , we have

$$\langle \text{vac} |_{\xi,1} = \frac{1}{\sqrt{2d^n(d^n + 1)}} \left( \langle 0 |^{\otimes n} + \langle 1 |^{\otimes n} \right), \quad (\text{S126})$$

$$\langle \text{vac} |_{\xi,0} \xi_{L,0} = \frac{1}{\sqrt{2d^n(d^n - 1)}} \left( \langle 0 |^{\otimes n} - \langle 1 |^{\otimes n} \right). \quad (\text{S127})$$

By the relationship  $M_{L,u}^{(2)} = V M_{L,u} V^{-1}$ , where  $V^\dagger |i_{\sigma_1} i_{\sigma_2} \dots i_{\sigma_n}\rangle = |\sigma_1 \sigma_2 \dots \sigma_n\rangle$ , we complete the proof of Theorem S2.

### 3. Proof for Corollary S3

We derive the spectral gap of  $u$ -structured local random circuits. Because  $\epsilon_k > \epsilon_{k'}$  for  $k > k'$ , the second largest eigenvalue of  $M_{L,u}^{(2)}$  in the even parity subspace is given by the two-particle state

$$\langle \text{vac} |_{\xi,1} \xi_{L,\frac{\pi}{n}} \xi_{L,-\frac{\pi}{n}} V, \quad (\text{S128})$$

where  $V^\dagger |i_{\sigma_1}, i_{\sigma_2}, \dots, i_{\sigma_n}\rangle = |\sigma_1, \sigma_2, \dots, \sigma_n\rangle$ , and the corresponding eigenvalue is

$$1 - \frac{2}{n} \epsilon_{\frac{\pi}{n}} = 1 - \frac{2e_u}{ne_H} \left( 1 - \frac{2d}{d^2+1} \cos \frac{\pi}{n} \right). \quad (\text{S129})$$

The second largest eigenvectors of  $M_{L,u}^{(2)}$  in the odd parity subspace are obtained by annihilating  $\xi_{L,0}$  and creating one of the two eigenmodes  $\xi_{L,\frac{2m\pi}{n}}$  and  $\xi_{L,-\frac{2m\pi}{n}}$ , and the eigenvectors are

$$\langle \text{vac} |_{\xi,0} \xi_{L,\frac{2\pi}{n}} V, \quad (\text{S130})$$

$$\langle \text{vac} |_{\xi,0} \xi_{L,-\frac{2\pi}{n}} V, \quad (\text{S131})$$

and the corresponding eigenvalue is

$$1 - \frac{1}{n} (\epsilon_0 + \epsilon_{\frac{2\pi}{n}}) = 1 - \frac{e_u(d-1)}{n(d+1)} - \frac{e_u}{ne_H} \left( 1 - \frac{2d}{d^2+1} \cos \frac{2\pi}{n} \right). \quad (\text{S132})$$

By comparing Eq. (S132) with Eq. (S129), because  $\cos k > \frac{1}{2}(1 + \cos 2k)$  for  $0 < k < \pi$ , we find that the second largest eigenvalue of  $M_{L,u}^{(2)}$  is given by Eq. (S129). On the other hand, the least eigenvalue is lower-bounded by filling all fermionic eigenmodes, and the eigenvalue is

$$\begin{aligned} & 1 - \frac{1}{n} \sum_k \frac{e_u}{e_H} \left( 1 - \frac{2d}{d^2+1} \cos k \right), \\ & = 1 - \frac{e_u}{e_H}, \end{aligned} \quad (\text{S133})$$

which is a negative number when  $e_u > e_H$ , and the absolute value is less than or equal to Eq. (S129) for any  $n \geq 2$ . Therefore, with the fact that the largest eigenvalue of the moment operator is 1, the spectral gap of  $M_{L,u}^{(2)}$  is  $\frac{2e_u}{ne_H} \left( 1 - \frac{2d}{d^2+1} \cos \frac{\pi}{n} \right)$ .

## B. Brick-wall circuits

Here, we diagonalize the moment operator of  $u$ -structured brick-wall random circuits  $M_{B,u}^{(2)}$ . We note that the diagonalization of matchgate brick-wall circuits has been recently considered in Ref. [71], which considers a similar circuit to ours.

### 1. Proof for Theorem S5

As with the previous section, we have the matrix form

$$\mathbf{M}_{B,u} = \sum_{\sigma_1, \dots, \sigma_n, \tau_1, \dots, \tau_n} \langle \sigma_1, \sigma_2, \dots, \sigma_n | M_{B,u}^{(2)} | \tilde{\tau}_1, \tilde{\tau}_2, \dots, \tilde{\tau}_n \rangle | i_{\sigma_1}, i_{\sigma_2}, \dots, i_{\sigma_n} \rangle \langle i_{\tau_1}, i_{\tau_2}, \dots, i_{\tau_n} |. \quad (\text{S134})$$

Under the solvable condition, the matrix  $\mathbf{M}_{B,u}$  consists of the  $4 \times 4$  matrix

$$\mathbf{W}^u = \begin{pmatrix} 1 & 0 & 0 & 0 \\ a & b' & 0 & a \\ a & 0 & b' & a \\ 0 & 0 & 0 & 1 \end{pmatrix}, \quad (\text{S135})$$

where we have used the assumption  $W^u(ISSI) = 0$  and defined  $a = \frac{d}{d^2+1} \frac{e_u}{e_H}$  and  $b' = 1 - \frac{e_u}{e_H}$ . By taking the logarithm of the matrix, we obtain

$$\log \mathbf{W}^u = \begin{pmatrix} 0 & 0 & 0 & 0 \\ x & y & 0 & x \\ x & 0 & y & x \\ 0 & 0 & 0 & 0 \end{pmatrix}, \quad (\text{S136})$$

where

$$\begin{aligned} x &= \frac{a \log b'}{b' - 1} \\ &= -\frac{d}{d^2 + 1} \log \left( 1 - \frac{e_u}{e_H} \right), \end{aligned} \quad (\text{S137})$$

$$\begin{aligned} y &= \log b' \\ &= \log \left( 1 - \frac{e_u}{e_H} \right), \end{aligned} \quad (\text{S138})$$

and we have  $\frac{x}{y} = -\frac{d}{d^2+1}$ . We then expand Eq. (S136) by the Pauli matrices as

$$\begin{aligned} \log \mathbf{W}^u &= y \frac{I \otimes I - Z \otimes Z}{2} + x(I \otimes X + X \otimes I) \frac{I \otimes I + Z \otimes Z}{2} \\ &= \frac{y}{2}(I \otimes I - Z \otimes Z) + \frac{x}{2}(I \otimes X + X \otimes I - iY \otimes Z - iZ \otimes Y). \end{aligned} \quad (\text{S139})$$

Here, to take the logarithm, we assumed that  $e_u > 0$  and  $e_u \neq e_H$ . For a negative number  $z$ , we take the value  $\log(z) = \log(|z|) + i\pi$ . We note that since  $M_{B,u}^{(2)}$  is continuous at  $e_u = e_H$ , the eigenvalues and eigenvectors of  $M_{B,H}^{(2)}$  are given by the results in this section after substituting  $e_H$  for  $e_u$ . We map the Pauli strings in Eq. (S139) to quadratic fermionic operators by the Jordan-Wigner transformation and Eq. (S139), we obtain

$$\begin{aligned} \log \mathbf{W}_{1,2}^u &= \frac{y}{2} \left( 1 - (c_1^\dagger - c_1)(c_2^\dagger + c_2) \right) + \frac{x}{2} \left( 2 - 2c_1^\dagger c_1 - 2c_2^\dagger c_2 - (c_1^\dagger + c_1)(c_2^\dagger + c_2) - (c_1^\dagger - c_1)(c_2^\dagger - c_2) \right) \\ &= \frac{y}{2} + x - x(c_1^\dagger c_1 + c_2^\dagger c_2) - \frac{y}{2} c_1^\dagger c_2 - \frac{y}{2} c_2^\dagger c_1 - \left( x + \frac{y}{2} \right) c_1^\dagger c_2^\dagger + \left( x - \frac{y}{2} \right) c_2 c_1. \end{aligned} \quad (\text{S140})$$

We define the number operator as  $N = \sum_{j=1}^{2n} c_j^\dagger c_j$  and the odd (even) parity subspace as the subspace spanned by the eigenvectors of  $N$  with odd (even) eigenvalues. The matrix  $M_{B,u}$  has the form

$$M_{B,u} = T_2 T_1, \quad (\text{S141})$$

where the matrix  $T_1$  and  $T_2$  are the first and the second layer of brick-wall random circuits, respectively.

Since  $(-1)^n$  commutes with the transfer matrix, we consider two subspaces with even and odd fermion number separately. By the Jordan-Wigner transformation, they are written as

$$\begin{aligned} T_1 &= \exp \left[ \frac{yn}{4} + \frac{xn}{2} - \sum_{j=1}^{\frac{n}{2}} \left( x(c_{2j-1}^\dagger c_{2j-1} + c_{2j}^\dagger c_{2j}) + \frac{y}{2}(c_{2j-1}^\dagger c_{2j} + c_{2j}^\dagger c_{2j-1}) \right. \right. \\ &\quad \left. \left. + \left( x + \frac{y}{2} \right) c_{2j-1}^\dagger c_{2j}^\dagger - \left( x - \frac{y}{2} \right) c_{2j} c_{2j-1} \right) \right], \end{aligned} \quad (\text{S142})$$

$$\begin{aligned} T_2 &= \exp \left[ \sum_{j=1}^{\frac{n}{2}} \left( \frac{y}{2} + x - x(c_{2j-1}^\dagger c_{2j-1} + c_{2j}^\dagger c_{2j}) - \frac{y}{2} c_{2j}^\dagger c_{2j+1} - \frac{y}{2} c_{2j+1}^\dagger c_{2j} \right. \right. \\ &\quad \left. \left. - \left( x + \frac{y}{2} \right) c_{2j}^\dagger c_{2j+1}^\dagger + \left( x - \frac{y}{2} \right) c_{2j+1} c_{2j} \right) \right], \end{aligned} \quad (\text{S143})$$

where, as with the case of local random circuits, we impose the anti-periodic boundary condition  $c_{n+1} = -c_1$ , if  $T_2$  acts on the even parity subspace, and periodic boundary conditions  $c_{n+1} = c_1$ , if  $T_2$  acts on the odd parity subspace.

Because of the (2-site) translation symmetry of the matrices, we use the discrete Fourier-transform of the creation operators in  $T_1$  and  $T_2$ : for  $j = 1, 2, \dots, n$ ,

$$c_j^\dagger = \frac{1}{\sqrt{n}} \sum_k e^{ikj} \eta_k^\dagger, \quad (\text{S144})$$

where  $k$  is summed over  $K_1$  when  $T_{1,2}$  acts on the odd subspace, and it is summed over  $K_0$  when  $T_{1,2}$  acts on the even subspace. We can translate each term in Eqs. (S142) and (S143) into the quadratic form of  $\{\eta_k\}$ , for example,

$$\begin{aligned} \sum_{j=1}^n c_{2j-1}^\dagger c_{2j-1} &= \frac{1}{2} \sum_{k,k' \in K_p} \left( \frac{1}{n} \sum_{j=1}^n e^{i(k-k') \cdot 2j} \right) e^{-i(k-k')} \eta_k^\dagger \eta_{k'} \\ &= \frac{1}{2} \sum_{k,k' \in K_p} \left( \delta_{k,k'} + \delta_{k-\pi,k'} \right) e^{-i(k-k')} \eta_k^\dagger \eta_{k'} \\ &= \frac{1}{2} \sum_{k \in K_p} \left( \eta_k^\dagger \eta_k - \eta_k^\dagger \eta_{k-\pi} \right), \end{aligned} \quad (\text{S145})$$

where the set  $K_1$  or  $K_0$  is chosen according to the parity of the subspace on which the fermionic operator acts. We then obtain

$$\begin{aligned} T_{1,p} = \exp \left[ \frac{yn}{4} + \frac{xn}{2} - \sum_{k \in K_p} \left( (x + \frac{y}{2} \cos k) \eta_k^\dagger \eta_k + \frac{y}{4} (e^{-ik} \eta_k^\dagger \eta_{k-\pi} + e^{ik} \eta_{k-\pi}^\dagger \eta_k) \right. \right. \\ \left. \left. + \frac{1}{4} (2x + y) e^{-ik} (\eta_k^\dagger \eta_{-k}^\dagger + \eta_k^\dagger \eta_{\pi-k}^\dagger) - \frac{1}{4} (2x - y) e^{ik} (\eta_{-k} \eta_k + \eta_{\pi-k} \eta_k) \right) \right], \end{aligned} \quad (\text{S146})$$

$$\begin{aligned} T_{2,p} = \exp \left[ \frac{yn}{4} + \frac{xn}{2} - \sum_{k \in K_p} \left( (x + \frac{y}{2} \cos k) \eta_k^\dagger \eta_k - \frac{y}{4} (e^{-ik} \eta_k^\dagger \eta_{k-\pi} + e^{ik} \eta_{k-\pi}^\dagger \eta_k) \right. \right. \\ \left. \left. + \frac{1}{4} (2x + y) e^{-ik} (\eta_k^\dagger \eta_{-k}^\dagger - \eta_k^\dagger \eta_{\pi-k}^\dagger) - \frac{1}{4} (2x - y) e^{ik} (\eta_{-k} \eta_k - \eta_{\pi-k} \eta_k) \right) \right], \end{aligned} \quad (\text{S147})$$

where the upper and lower signs in the above equations correspond to the even and odd parity subspaces, respectively, on which the moment operator acts. We can rewrite it by summing only over the non-negative values in  $K_p$ , and we have

$$\begin{aligned} T_{1,p} = \exp \left[ \frac{yn}{4} + \frac{xn}{2} - \sum_{0 < k < \pi: k \in K_p} \left( (x + \frac{y}{2} \cos k) (\eta_k^\dagger \eta_k + \eta_{-k}^\dagger \eta_{-k}) - i \frac{y}{2} \sin k (\eta_k^\dagger \eta_{k-\pi} - \eta_{k-\pi}^\dagger \eta_k) \right. \right. \\ - \frac{i}{2} (2x + y) \sin k \eta_k^\dagger \eta_{-k}^\dagger + \frac{1}{4} (2x + y) (e^{-ik} \eta_k^\dagger \eta_{\pi-k}^\dagger + e^{ik} \eta_{-k}^\dagger \eta_{k-\pi}^\dagger) \\ - \frac{i}{2} (2x - y) \sin k \eta_{-k} \eta_k - \frac{1}{4} (2x - y) (e^{ik} \eta_{\pi-k} \eta_k + e^{-ik} \eta_{k-\pi} \eta_{-k}) \\ \left. \left. - \frac{\delta_p}{2} \left( (2x + y) (\eta_0^\dagger \eta_0 + \eta_0^\dagger \eta_\pi^\dagger) + (2x - y) (\eta_\pi^\dagger \eta_\pi - \eta_\pi \eta_0) \right) \right) \right], \end{aligned} \quad (\text{S148})$$

$$\begin{aligned} T_{2,p} = \exp \left[ \frac{yn}{4} + \frac{xn}{2} - \sum_{0 < k < \pi: k \in K_p} \left( (x + \frac{y}{2} \cos k) (\eta_k^\dagger \eta_k + \eta_{-k}^\dagger \eta_{-k}) + i \frac{y}{2} \sin k (\eta_k^\dagger \eta_{k-\pi} - \eta_{k-\pi}^\dagger \eta_k) \right. \right. \\ - \frac{i}{2} (2x + y) \sin k \eta_k^\dagger \eta_{-k}^\dagger - \frac{1}{4} (2x + y) (e^{-ik} \eta_k^\dagger \eta_{\pi-k}^\dagger + e^{ik} \eta_{-k}^\dagger \eta_{k-\pi}^\dagger) \\ - \frac{i}{2} (2x - y) \sin k \eta_{-k} \eta_k + \frac{1}{4} (2x - y) (e^{ik} \eta_{\pi-k} \eta_k + e^{-ik} \eta_{k-\pi} \eta_{-k}) \\ \left. \left. - \frac{\delta_p}{2} \left( (2x + y) (\eta_0^\dagger \eta_0 - \eta_0^\dagger \eta_\pi^\dagger) + (2x - y) (\eta_\pi^\dagger \eta_\pi + \eta_\pi \eta_0) \right) \right) \right], \end{aligned} \quad (\text{S149})$$

where  $\delta_p = 1 - p$ . Furthermore, we can only sum over the first half of the non-negative values in  $K_p$ , and we have

$$T_{1,p} = \exp \left[ - \sum_{0 < k < \frac{\pi}{2}: k \in K_p} S_{1,k} - \frac{\delta_p}{2} S_{1,0} - \frac{\delta_{p,n}}{2} S_{1,\frac{\pi}{2}} \right], \quad (\text{S150})$$

$$T_{2,p} = \exp \left[ - \sum_{0 < k < \frac{\pi}{2}: k \in K_p} S_{2,k} - \frac{\delta_p}{2} S_{2,0} - \frac{\delta_{p,n}}{2} S_{2,\frac{\pi}{2}} \right], \quad (\text{S151})$$

where  $\delta_{p,n} = \frac{1+(-1)^{p+n}}{2}$  and we have defined

$$\begin{aligned} S_{1,k} = & -2x - y + \left(x + \frac{y}{2} \cos k\right) (\eta_k^\dagger \eta_k + \eta_{-k}^\dagger \eta_{-k}) + \left(x - \frac{y}{2} \cos k\right) (\eta_{\pi-k}^\dagger \eta_{\pi-k} + \eta_{k-\pi}^\dagger \eta_{k-\pi}) \\ & + i \frac{y}{2} \sin k (-\eta_k^\dagger \eta_{k-\pi} + \eta_{k-\pi}^\dagger \eta_k - \eta_{\pi-k}^\dagger \eta_{-k} + \eta_{-k}^\dagger \eta_{\pi-k}) \\ & - \frac{i}{2} (2x + y) \sin k (\eta_k^\dagger \eta_{-k} + \eta_{\pi-k}^\dagger \eta_{k-\pi}) + \frac{1}{2} (2x + y) \cos k (\eta_k^\dagger \eta_{\pi-k} + \eta_{-k}^\dagger \eta_{k-\pi}) \\ & - \frac{i}{2} (2x - y) \sin k (\eta_{-k} \eta_k + \eta_{k-\pi} \eta_{\pi-k}) - \frac{1}{2} (2x - y) \cos k (\eta_{\pi-k} \eta_k + \eta_{k-\pi} \eta_{-k}), \end{aligned} \quad (\text{S152})$$

$$S_{1,0} = -2x - y + (2x + y) (\eta_0^\dagger \eta_0 + \eta_0^\dagger \eta_\pi) + (2x - y) (\eta_\pi^\dagger \eta_\pi - \eta_\pi \eta_0), \quad (\text{S153})$$

$$\begin{aligned} S_{1,\frac{\pi}{2}} = & -2x - y + 2x (\eta_{\frac{\pi}{2}}^\dagger \eta_{\frac{\pi}{2}} + \eta_{-\frac{\pi}{2}}^\dagger \eta_{-\frac{\pi}{2}}) - iy (\eta_{\frac{\pi}{2}}^\dagger \eta_{-\frac{\pi}{2}} - \eta_{-\frac{\pi}{2}}^\dagger \eta_{\frac{\pi}{2}}) \\ & - i(2x + y) \eta_{\frac{\pi}{2}}^\dagger \eta_{-\frac{\pi}{2}}^\dagger - i(2x - y) \eta_{-\frac{\pi}{2}} \eta_{\frac{\pi}{2}}, \end{aligned} \quad (\text{S154})$$

$$\begin{aligned} S_{2,k} = & -2x - y + \left(x + \frac{y}{2} \cos k\right) (\eta_k^\dagger \eta_k + \eta_{-k}^\dagger \eta_{-k}) + \left(x - \frac{y}{2} \cos k\right) (\eta_{\pi-k}^\dagger \eta_{\pi-k} + \eta_{k-\pi}^\dagger \eta_{k-\pi}) \\ & - i \frac{y}{2} \sin k (-\eta_k^\dagger \eta_{k-\pi} + \eta_{k-\pi}^\dagger \eta_k - \eta_{\pi-k}^\dagger \eta_{-k} + \eta_{-k}^\dagger \eta_{\pi-k}) \\ & - \frac{i}{2} (2x + y) \sin k (\eta_k^\dagger \eta_{-k} + \eta_{\pi-k}^\dagger \eta_{k-\pi}) - \frac{1}{2} (2x + y) \cos k (\eta_k^\dagger \eta_{\pi-k} + \eta_{-k}^\dagger \eta_{k-\pi}) \\ & - \frac{i}{2} (2x - y) \sin k (\eta_{-k} \eta_k + \eta_{k-\pi} \eta_{\pi-k}) + \frac{1}{2} (2x - y) \cos k (\eta_{\pi-k} \eta_k + \eta_{k-\pi} \eta_{-k}), \end{aligned} \quad (\text{S155})$$

$$S_{2,0} = -2x - y + (2x + y) (\eta_0^\dagger \eta_0 - \eta_0^\dagger \eta_\pi) + (2x - y) (\eta_\pi^\dagger \eta_\pi + \eta_\pi \eta_0), \quad (\text{S156})$$

$$\begin{aligned} S_{2,\frac{\pi}{2}} = & -2x - y + 2x (\eta_{\frac{\pi}{2}}^\dagger \eta_{\frac{\pi}{2}} + \eta_{-\frac{\pi}{2}}^\dagger \eta_{-\frac{\pi}{2}}) + iy (\eta_{\frac{\pi}{2}}^\dagger \eta_{-\frac{\pi}{2}} - \eta_{-\frac{\pi}{2}}^\dagger \eta_{\frac{\pi}{2}}) \\ & - i(2x + y) \eta_{\frac{\pi}{2}}^\dagger \eta_{-\frac{\pi}{2}}^\dagger - i(2x - y) \eta_{-\frac{\pi}{2}} \eta_{\frac{\pi}{2}}. \end{aligned} \quad (\text{S157})$$

Because of the commutation relations  $[S_{i,k}, S_{j,k'}] = 0$  when  $k \neq k'$ , the matrix  $M_{B,u}$  is decomposed into  $M_{B,u} = \prod_k e^{-S_{2,k}} e^{-S_{1,k}}$ . For each  $k \in K_p$  satisfying  $0 < k < \frac{\pi}{2}$ , we define the following row and column vectors

$$\boldsymbol{\eta}_k = (\eta_k^\dagger \eta_{-k} \eta_{k-\pi}^\dagger \eta_{\pi-k}), \quad (\text{S158})$$

$$\boldsymbol{\eta}_k^\dagger = (\eta_k \eta_{-k}^\dagger \eta_{k-\pi} \eta_{\pi-k}^\dagger)^\top, \quad (\text{S159})$$

whose  $i$ -th elements are denoted by  $\eta_{k,i}$  and  $\eta_{k,i}^\dagger$ , respectively, for  $i \in \{1, 2, 3, 4\}$ . So as to diagonalize  $M_{B,u}$ , we consider the adjoint action of  $M_{B,u}$  on  $\boldsymbol{\eta}_k$  and  $\boldsymbol{\eta}_k^\dagger$ . From the relationship  $e^{-S_{k,m}} \boldsymbol{\eta}_{k,i}^\dagger e^{S_{m,k}} = \sum_{j=1}^4 (e^{S_{m,k}})_{i,j} \boldsymbol{\eta}_{k,j}^\dagger$ , for  $m \in \{1, 2\}$  and a matrix  $\mathcal{S}_{m,k}$ , to be defined later, we find that for each  $k \in K_p$  satisfying  $0 < k < \frac{\pi}{2}$ ,

$$M_{B,u}^{-1} \boldsymbol{\eta}_{k,i} M_{B,u} = \sum_{j=1}^4 \eta_{k,j} \mathcal{M}_{k,ji}, \quad (\text{S160})$$

$$M_{B,u} \boldsymbol{\eta}_{k,i}^\dagger M_{B,u}^{-1} = \sum_{j=1}^4 \mathcal{M}_{k,ij} \boldsymbol{\eta}_{k,j}^\dagger, \quad (\text{S161})$$

where the matrix  $\mathcal{M}_k = (\mathcal{M}_{k,ij})_{ij}$  is written in the form  $\mathcal{M}_k = e^{\mathcal{S}_{2,k}} e^{\mathcal{S}_{1,k}}$ , with

$$\mathcal{S}_{1,k} = \frac{1}{2} \begin{pmatrix} 2x + y \cos k & -i(2x + y) \sin k & -iy \sin k & (2x + y) \cos k \\ -i(2x - y) \sin k & -2x - y \cos k & (2x - y) \cos k & iy \sin k \\ iy \sin k & -(2x + y) \cos k & 2x - y \cos k & i(2x + y) \sin k \\ -(2x - y) \cos k & -iy \sin k & i(2x - y) \sin k & -2x + y \cos k \end{pmatrix}, \quad (\text{S162})$$

$$\mathcal{S}_{2,k} = \frac{1}{2} \begin{pmatrix} 2x + y \cos k & -i(2x + y) \sin k & iy \sin k & -(2x + y) \cos k \\ -i(2x - y) \sin k & -2x - y \cos k & -(2x - y) \cos k & -iy \sin k \\ -iy \sin k & (2x + y) \cos k & 2x - y \cos k & i(2x + y) \sin k \\ (2x - y) \cos k & iy \sin k & i(2x - y) \sin k & -2x + y \cos k \end{pmatrix}. \quad (\text{S163})$$

The matrix  $\mathcal{M}_k$  is diagonalized as  $\mathcal{M}_k = W_k \Lambda_k W_k^{-1}$ , where  $\Lambda_k$  is the diagonal matrix with the following diagonal elements, corresponding to the eigenvalues of  $\mathcal{M}_k$ ,

$$\lambda'_k = e^y \left( q_k + \sqrt{q_k^2 + 1} \right)^2, \quad (\text{S164})$$

$$\lambda'_{\pi-k} = e^y \left( q_k - \sqrt{q_k^2 + 1} \right)^2, \quad (\text{S165})$$

$$\lambda'_{k-\pi} = e^{-y} \left( q_k + \sqrt{q_k^2 + 1} \right)^2, \quad (\text{S166})$$

$$\lambda'_{-k} = e^{-y} \left( q_k - \sqrt{q_k^2 + 1} \right)^2, \quad (\text{S167})$$

where the parameter  $q_k$  is

$$\begin{aligned} q_k &= \frac{2x \sinh\left(\frac{y}{2}\right) \cos k}{y} \\ &= \frac{d \cos k e_u}{\sqrt{(d^4 - 1)(e_H - e_u)}}. \end{aligned} \quad (\text{S168})$$

This diagonalization is proven in Sec. S7. We remark that  $q_k$  is a non-real numbers when  $e_u > e_H$ , and the eigenvalues can also be non-real in this regime. We find that the diagonalizing matrix  $W_k$ , for each  $k \in K_p$  satisfying  $0 < k < \frac{\pi}{2}$ , is

$$W_k = \begin{pmatrix} 1 & 1 & 1 & 1 \\ iz \tan \frac{k}{2} & iz \tan \frac{k}{2} & -i \cot \frac{k}{2} & -i \cot \frac{k}{2} \\ -ir_{1,k} \tan \frac{k}{2} & -ir_{2,k} \tan \frac{k}{2} & -ir_{2,k} \cot \frac{k}{2} & -ir_{1,k} \cot \frac{k}{2} \\ -zr_{1,k} & -zr_{2,k} & r_{2,k} & r_{1,k} \end{pmatrix}, \quad (\text{S169})$$

where we have defined

$$z = \frac{y - 2x}{y + 2x}, \quad (\text{S170})$$

$$r_{i,k} = \frac{y(\cosh \frac{y}{2} + (-1)^i \sqrt{1 + q_k^2})}{(y - 2x \cos k) \sinh \frac{y}{2}}, \quad \text{for } i \in \{1, 2\}. \quad (\text{S171})$$

In terms of  $d$  and  $e_u$ , they are expressed as

$$z = \left( \frac{d + 1}{d - 1} \right)^2, \quad (\text{S172})$$

$$r_{i,k} = \frac{e_u - 2e_H - (-1)^i 2\sqrt{e_H(e_H - e_u) + a_H^2 e_u^2 \cos^2 k}}{e_u(1 + 2a_H \cos k)}, \quad \text{for } i \in \{1, 2\}, \quad (\text{S173})$$

where we have defined  $a_H = \frac{d}{d^2 + 1}$ . We note that the matrix  $W_k$  depends on  $e_u$ , and it is in contrast to the diagonalizing matrix for local random circuits Eq. (S106), which does not. We can construct the left and right eigenmodes of  $M_{B,u}$  by

$$(\zeta_{L,k} \zeta_{L,\pi-k} \zeta_{L,k-\pi} \zeta_{L,k}) = \boldsymbol{\eta}_k W_k, \quad (\text{S174})$$

$$(\zeta_{R,k}^\dagger \zeta_{R,\pi-k}^\dagger \zeta_{R,k-\pi}^\dagger \zeta_{R,-k}^\dagger)^\top = W_k^{-1} \boldsymbol{\eta}_k^\dagger, \quad (\text{S175})$$



which satisfy

$$M_{B,u}^{-1} \zeta_{L,l} M_{B,u} = \lambda_l \zeta_{L,l}, \quad (\text{S176})$$

$$M_{B,u} \zeta_{R,l}^\dagger M_{B,u}^{-1} = \lambda_l \zeta_{R,l}^\dagger, \quad (\text{S177})$$

for  $l \in \{k, -k, k - \pi, \pi - k\}$ .

Likewise, we obtain the eigenvalue and the eigenmodes of the adjoint action of  $M_{B,u}$  restricted to the subspace of  $k = 0, \pi$  and  $k = \frac{\pi}{2}, -\frac{\pi}{2}$ . In the subspace of  $k = 0, \pi$ , we find that the eigenmodes are  $(\zeta_{L,0} \zeta_{L,\pi}) = \boldsymbol{\eta}_0 W_0$  and  $(\zeta_{R,0}^\dagger \zeta_{R,\pi}^\dagger)^\top = W_0^{-1} \boldsymbol{\eta}_0^\dagger$ , where  $\boldsymbol{\eta}_0 = (\eta_0^\dagger \eta_\pi)$  and

$$W_0 = \begin{pmatrix} -r_{1,0} & -r_{2,0} \\ 1 & 1 \end{pmatrix}, \quad (\text{S178})$$

and the corresponding eigenvalues are

$$\lambda_0 = e^y \left( q_0 + \sqrt{q_0^2 + 1} \right)^2, \quad (\text{S179})$$

$$\lambda_\pi = e^y \left( q_0 - \sqrt{q_0^2 + 1} \right)^2. \quad (\text{S180})$$

In the subspace of  $k = \frac{\pi}{2}, -\frac{\pi}{2}$ , we find that the eigenmodes are  $(\zeta_{L,\frac{\pi}{2}} \zeta_{L,-\frac{\pi}{2}}) = \boldsymbol{\eta}_{\frac{\pi}{2}} W_{\frac{\pi}{2}}$  and  $(\zeta_{R,\frac{\pi}{2}}^\dagger \zeta_{R,-\frac{\pi}{2}}^\dagger)^\top = W_{\frac{\pi}{2}}^{-1} \boldsymbol{\eta}_{\frac{\pi}{2}}^\dagger$ , where  $\boldsymbol{\eta}_{\frac{\pi}{2}} = (\eta_{\frac{\pi}{2}}^\dagger \eta_{-\frac{\pi}{2}})$  and

$$W_{\frac{\pi}{2}} = \begin{pmatrix} i & iz^{-1} \\ 1 & 1 \end{pmatrix}, \quad (\text{S181})$$

and the corresponding eigenvalues are

$$\lambda'_{\frac{\pi}{2}} = e^y, \quad (\text{S182})$$

$$\lambda'_{-\frac{\pi}{2}} = e^{-y}. \quad (\text{S183})$$

Once we obtain the vacuum  $|\text{vac}\rangle_{\zeta,p}$ , which satisfy  $\langle \text{vac} |_{\zeta,p} \zeta_{R,l}^\dagger = 0$  and  $\zeta_{L,l} |\text{vac}\rangle_{\zeta,p} = 0$  with  $p = 0$  ( $p = 1$ ) for the odd (even) parity subspace, we find that the eigenvectors of  $M_{B,u}$  are of the form  $\langle \text{vac} |_{\zeta,p} \prod_{k \in K'} \zeta_{L,k}$  and  $\prod_{k \in K'} \zeta_{R,k}^\dagger |\text{vac}\rangle_{\zeta,p}$ , where  $K'$  is a subset of  $K_p$ . Now, we find the vacuum  $|\text{vac}\rangle_{\zeta,p}$ . We observe that  $\zeta_{R,l}^\dagger$ , for  $l \in \{k, -k, k - \pi, \pi - k\}$  and  $0 < k < \frac{\pi}{2}$ , consists only of the annihilation operators  $\eta_k, \eta_{k-\pi}$  and the creation operator  $\eta_{-k}^\dagger, \eta_{\pi-k}^\dagger, \zeta_{R,l}^\dagger$ , for  $l \in \{0, \pi\}$  consists only of  $\eta_0$  and  $\eta_\pi^\dagger$ , and  $\zeta_{R,l}^\dagger$ , for  $l \in \{\frac{\pi}{2}, -\frac{\pi}{2}\}$  consists only of  $\eta_{\frac{\pi}{2}}^\dagger$  and  $\eta_{-\frac{\pi}{2}}^\dagger$ , and we therefore find that

$$\langle \text{vac} |_{\eta,p} \eta_0^{\delta_p} \eta_{\frac{\pi}{2}}^{\delta_{p,n}} \left( \prod_{0 < k < \frac{\pi}{2}; k \in K_p} \eta_k \eta_{k-\pi} \right) \zeta_{R,l}^\dagger = 0 \quad (\text{S184})$$

for any  $l$ , where  $\langle \text{vac} |_{\eta,p}$  is the vacuum of  $\{\eta_k\}$  satisfying  $\langle \text{vac} |_{\eta,p} \eta_k^\dagger = 0$  for any  $k$ . Similarly, it holds that  $\zeta_{L,l} \left( \prod_{0 < k < \frac{\pi}{2}; k \in K_p} \eta_k^\dagger \eta_{k-\pi}^\dagger \right) \left( \eta_{\frac{\pi}{2}}^\dagger \right)^{\delta_{p,n}} \left( \eta_0^\dagger \right)^{\delta_p} |\text{vac}\rangle_{\eta,p} = 0$  for any  $l$ . Thus, we have

$$|\text{vac}\rangle_{\zeta,p} = \left( \prod_{0 < k < \frac{\pi}{2}; k \in K_p} \eta_k^\dagger \eta_{k-\pi}^\dagger \right) \left( \eta_{\frac{\pi}{2}}^\dagger \right)^{\delta_{p,n}} \left( \eta_0^\dagger \right)^{\delta_p} |\text{vac}\rangle_{\eta,p}. \quad (\text{S185})$$

It is easy to check that the vacuums in the even and odd parity subspaces,  $|\text{vac}\rangle_{\zeta,p}$ , are eigenvectors of  $M_{B,u}$  and the corresponding eigenvalues are  $e^{\frac{yn}{2}}$  and  $e^{\frac{yn}{2}-y}$  in the even and odd subspaces, respectively.

$M_{B,u}^{(2)}$  has two eigenvectors  $|I\rangle^{\otimes n}$  and  $|S\rangle^{\otimes n}$  with eigenvalue 1, and they are the only eigenvalue with absolute value 1 due to the Schur-Weyl duality and the fact that

$$\lim_{t \rightarrow \infty} \left( M_{B,u}^{(2)} \right)^t = M_H^{(2)} \quad (\text{S186})$$

for  $e_u \neq 0$ , where  $M_{\text{H}}^{(2)}$  is the moment operator of the  $n$ -qudit global Haar random unitaries. We rewrite these leading eigenvectors in terms of the eigenmodes, so as to construct subleading eigenvalues and eigenvectors. Because  $\lambda'_{k-\pi}\lambda'_{-k} = e^{-2y}$  for  $0 < k < \frac{\pi}{2}$ , the left eigenvectors of  $M_{B,u}$  with eigenvalue 1 are given by filling the half of fermions for  $-\pi < k < 0$ , namely,

$$\langle \psi_1 |_{\text{p}} = \langle \text{vac} |_{\zeta, \text{p}} \prod_{-\pi < k < 0: k \in K_p} \zeta_{L,k}, \quad (\text{S187})$$

where we have used that  $\langle \text{vac} |_{\zeta, \text{p}}$  is the eigenvectors of  $M_{B,u}$  with eigenvalue  $e^{\frac{y_n}{2} - \delta y}$ , and the upper and lower signs correspond to the even and odd subspaces, respectively. We can confirm that the parity of fermionic number of  $\langle \psi_1 |_{+}$  and  $\langle \psi_1 |_{-}$  are even and odd, respectively, from Eqs. (S174), (S185), and (S187). Furthermore, similarly as in the previous section, we can confirm by a straightforward calculation that Eq. (S187) is equal to  $\langle \psi_1 |_{\text{p}} = \langle 0 |^{\otimes n} \mp \langle 1 |^{\otimes n}$ , up to normalization coefficients.

Therefore, the left eigenvectors of  $M_{B,u}^{(2)}$  in the even parity subspace are

$$\left( \langle 0 |^{\otimes n} - \langle 1 |^{\otimes n} \right) \prod_{-\pi < k < 0: k \in K_1} \left( \zeta_{R,k}^{\dagger} \right)^{i_k} \prod_{0 < k < \pi: k \in K_1} \left( \zeta_{L,k} \right)^{i_k} V, \quad (\text{S188})$$

where  $V^{\dagger} |i_{\sigma_1}, i_{\sigma_2}, \dots, i_{\sigma_n}\rangle = |\sigma_1, \sigma_2, \dots, \sigma_n\rangle$ , and the corresponding eigenvalues are

$$\begin{aligned} & \left( \frac{1}{\lambda'_{-\frac{\pi}{2}}} \right)^{\delta_n i_{-\frac{\pi}{2}}} \left( \lambda'_{\frac{\pi}{2}} \right)^{\delta_n i_{\frac{\pi}{2}}} \prod_{0 < k < \frac{\pi}{2}: k \in K_1} \left( \frac{1}{\lambda'_{k-\pi}} \right)^{i_{k-\pi}} \left( \frac{1}{\lambda'_{-k}} \right)^{i_{-k}} \left( \lambda'_k \right)^{i_k} \left( \lambda'_{\pi-k} \right)^{i_{\pi-k}}, \\ & = \left( \lambda'_{\frac{\pi}{2}} \right)^{\delta_n \left( i_{\frac{\pi}{2}} + i_{-\frac{\pi}{2}} \right)} \prod_{0 < k < \frac{\pi}{2}: k \in K_1} \left( \lambda'_k \right)^{i_k + i_{-k}} \left( \lambda'_{\pi-k} \right)^{i_{\pi-k} + i_{k-\pi}}, \\ & = \prod_{k \in K_1} \left( \lambda_k \right)^{i_k} \end{aligned} \quad (\text{S189})$$

where, for  $0 < k \leq \frac{\pi}{2}$ , we have used  $\frac{1}{\lambda'_{-k}} = \lambda'_k$  and  $\frac{1}{\lambda'_{k-\pi}} = \lambda'_{\pi-k}$  in the first equality, and we have defined  $\lambda_k = \lambda_{-k} = \lambda'_k$  and  $\lambda_{\pi-k} = \lambda_{k-\pi} = \lambda'_{\pi-k}$  in the second equality. The eigenvectors and eigenvalues in the odd parity space are obtained similarly. By rewriting the eigenvalues and eigenvectors in terms of  $d$  and  $e_u$ , we have proven Theorem S4.

## 2. Proof for Corollary S5

We derive the spectral gap of  $u$ -structured brick-wall random circuits. Since the absolute value of the eigenvalues  $|\lambda_k|$  for  $k \in K_p$  satisfy  $|\lambda_k| \leq 1$ , and in particular  $|\lambda_k| < 1$  for non-identity gate  $u$ , the second-largest eigenvalue in absolute value is given by the maximum choice of filling two fermionic eigenmodes, that is,  $\max_{i,j \in K_p} (|\lambda_i \lambda_j|)$ . From Eqs. (S164) and (S165), we find that  $|\lambda_k| \geq |\lambda_{\pi-k}|$ , and moreover,  $|\lambda_k|$  is monotonically decreasing in  $k$  for  $0 \geq k \geq \frac{\pi}{2}$ . Thus, the second largest absolute values of the eigenvalues in the even and odd parity sectors are  $|\lambda_{\frac{\pi}{n}}|^2$  and  $\lambda_0 |\lambda_{\frac{2\pi}{n}}|$ , where we have used that  $\lambda_0$  is a real number for any integer  $d \geq 2$  and real number  $0 \leq e_u \leq \frac{d^2-1}{d^2}$ . Thus, we have

$$\max_{i,j \in K_p} (|\lambda_i \lambda_j|) = \max \left( |\lambda_{\frac{\pi}{n}}|^2, \lambda_0 |\lambda_{\frac{2\pi}{n}}| \right). \quad (\text{S190})$$

When  $|\lambda_{\frac{2\pi}{n}}|$  is real,  $|\lambda_{\frac{\pi}{n}}|$  is also real. In this case, because  $\lambda_k$  is a convex function in  $k$  when  $\lambda_k$  is real, we have  $(\lambda_{\frac{\pi}{n}})^2 \geq \lambda_0 \lambda_{\frac{2\pi}{n}}$ . On the other hand,  $\lambda_k$  can be a non-real number, for some  $0 < k \leq \frac{\pi}{2}$ , if the entangling power of  $u$  exceed the Haar random value,  $e_u > e_{\text{H}}$ . When  $\lambda_k$  is not real, it is easy to show from Eq. (S165) that  $|\lambda_k| = \frac{e_u}{e_{\text{H}}} - 1$ , which does not depend on  $k$ . Moreover, when  $\lambda_{\frac{\pi}{n}}$  is a non-real number, so is  $\lambda_{\frac{2\pi}{n}}$ , and thus in this case  $\max \left( |\lambda_{\frac{\pi}{n}}|^2, \lambda_0 |\lambda_{\frac{2\pi}{n}}| \right) = \lambda_0 |\lambda_{\frac{2\pi}{n}}| = \lambda_0 \left( \frac{e_u}{e_{\text{H}}} - 1 \right)$ , which completes the proof for Corollary S5.

## C. More global randomness: Proof for Theorem S1

More randomness with respect to positivity for structured local random circuits is proven in Sec. S5 A 1. We remark that under the solvable condition, since the eigenvectors of the moment operator do not depend on  $e_u$ , we also have

$$(M_{L,u}^{(2)})^t \Big|_{V_1^{\perp}} < (M_{L,\text{H}}^{(2)})^t \Big|_{V_1^{\perp}} \quad (\text{S191})$$

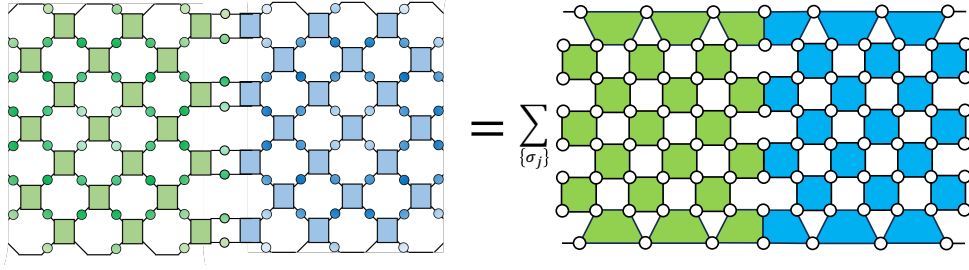


FIG. S2. The frame potential (left-hand side) and the classical spin model (right-hand side).

if  $e_u > e_H$ . Next, we prove more randomness with respect to the spectral gap. This follows immediately from Theorems S2 and S4 as follows. For a  $u$ -structured local random circuit, by Corollary S3, the spectral gap is given by  $\frac{2e_u}{ne_H} \left(1 - \frac{2d}{d^2+1}\right) \cos \frac{\pi}{n}$ , which implies that the gap is greater than that of local Haar random circuits if and only if  $e_u > e_H$ .

For a  $u$ -structured brick-wall circuit, when  $\lambda_{\frac{\pi}{n}}$  is a real number, it turns out that the value  $1 - (\lambda_{\frac{\pi}{n}})^2$  monotonically increases in  $e_u$ , where it is always real for any  $e_u \leq e_H$ . For local Haar random circuits, the spectral gap is obtained by plugging  $e_H$  for  $e_u$ , and it is  $1 - \left(\frac{d}{d^2+1}\right)^4 (2 \cos \frac{2\pi}{n} + 2)$ . Then, when  $\lambda_{\frac{2\pi}{n}}$  is a non-real number, it is also shown by a straightforward calculation that

$$1 - \lambda_{\pi} \lambda_{\pi - \frac{2\pi}{n}} = 1 - \lambda_{\pi} \left(\frac{e_u}{e_H} - 1\right) > 1 - \left(\frac{d}{d^2+1}\right)^4 \left(2 \cos \frac{2\pi}{n} + 2\right) \quad (\text{S192})$$

for  $e_H < e_u \leq 1$ . Therefore the gap of  $u$ -structured brick-wall circuits is larger than that of brick-wall Haar random circuits if and only if  $e_u > e_H$ .

## S6. FRAME POTENTIAL

The  $k$ -th frame potential [41] of random circuits  $\nu$  with the circuit depth  $t$  is defined by

$$F_{\nu_t}^{(k)} = \int |\text{Tr}(U^\dagger V)|^{2k} d\nu_t(U) d\nu_t(V). \quad (\text{S193})$$

Equivalently, we can rewrite it in terms of the moment operator as

$$F_{\nu_t}^{(k)} = \text{Tr} \left[ \left( M_{\nu}^{(k)} \right)^t \cdot \left( M_{\nu}^{(k)\dagger} \right)^t \right]. \quad (\text{S194})$$

From our diagonalization results in the main text, we can obtain the exact value of the second frame potential in principle, since we have obtained all eigenvalues and eigenvectors. However, the exact formula for the frame potential involves  $t$ -th power summation of eigenvalues and it might not be concise. In this section, we obtain the upper-bound on the frame potential of  $u$ -structured brick-wall circuits with slight modification, by the standard technique of mapping to partition functions of Ising-like model [16, 81]. It gives a more concise formula than merely  $t$ -th power summation of eigenvalues.

### A. Second-frame potential

We consider the case of  $k = 2$ . The frame potential of the ensemble of local random circuits can be mapped to the partition function of a corresponding Ising model. This mapping has been studied for random circuits with Haar random two-qudit gates to calculate the entanglement entropy [85] and the frame potential [81]. We average each single-qudit gate over Haar measure in Eq. (S193), and from Eq. (S12), we have for each two-qudit gate

$$\begin{aligned} & \int \left( (v_3 \otimes v_4) u_{i,i+1} (v_1 \otimes v_2) \right)^{\otimes 2,2} d\mu_H(v_1) d\mu_H(v_2) d\mu_H(v_3) d\mu_H(v_4) \\ &= \sum_{\sigma_1, \sigma_2, \sigma_3, \sigma_4 \in S_2} \left( |\tilde{\sigma}_3\rangle \langle \sigma_3| \otimes |\tilde{\sigma}_4\rangle \langle \sigma_4| \right) u_{i,i+1}^{\otimes 2,2} \left( |\tilde{\sigma}_1\rangle \langle \sigma_1| \otimes |\tilde{\sigma}_2\rangle \langle \sigma_2| \right)' \end{aligned} \quad (\text{S195})$$

Then, Eq. (S193) is equal to the partition function of the classical statistical mechanics model consisting of  $k$ -state spins (Fig. S6 A), where the states are  $\{\sigma_i\}_{i=1,\dots,k}$ , and the four-body Boltzmann weights are obtained by

$$W^u(\sigma_1\sigma_2\sigma_3\sigma_4) = (\langle\sigma_3| \otimes \langle\sigma_4|) u^{\otimes 2,2} (|\tilde{\sigma}_1\rangle \otimes |\tilde{\sigma}_2\rangle). \quad (\text{S196})$$

Graphically, the weights are

$$\begin{array}{c} \textcircled{\sigma_1} \textcircled{I} \\ \textcircled{\sigma_2} \textcircled{I} \end{array} = \begin{cases} 1 & (\sigma_1 = \sigma_2 = I), \\ 0 & \text{otherwise,} \end{cases} \quad (\text{S197})$$

$$\begin{array}{c} \textcircled{I} \textcircled{\sigma_3} \\ \textcircled{I} \textcircled{\sigma_4} \end{array} = \frac{1}{(d^2 - 1)^2} \left( d^3 + d - \frac{\langle\sigma_3| \otimes \langle\sigma_4| u^{\otimes 2,2} |S\rangle \otimes |I\rangle}{d} - \frac{\langle\sigma_3| \otimes \langle\sigma_4| u^{\otimes 2,2} |I\rangle \otimes |S\rangle}{d} \right), \quad (\text{S198})$$

$$\begin{array}{c} \textcircled{S} \textcircled{\sigma_3} \\ \textcircled{I} \textcircled{\sigma_4} \end{array} = \frac{1}{(d^2 - 1)^2} \left( -2d^2 + \langle\sigma_3| \otimes \langle\sigma_4| u^{\otimes 2,2} |S\rangle \otimes |I\rangle + \frac{\langle\sigma_3| \otimes \langle\sigma_4| u^{\otimes 2,2} |I\rangle \otimes |S\rangle}{d^2} \right), \quad (\text{S199})$$

for  $\sigma_3 \neq \sigma_4$  where we have used the facts on the matrix elements in Sec. S2 C. Other weights are obtained by the spin-flip symmetry  $W(\sigma_1\sigma_2\sigma_3\sigma_4) = W(\bar{\sigma}_1\bar{\sigma}_2\bar{\sigma}_3\bar{\sigma}_4)$ , where  $\bar{I} = S$  and  $\bar{S} = I$ .

### B. Frame potential in single-domain wall sector

We consider a structured circuit in which we apply two distinct layers alternatively, which is a slightly different model from what we have considered in Sec. S4. Specifically, we consider an analytically tractable case where the interaction in the layers at an odd time (blue triangles in Eq. (S200)) satisfies the 2-design condition, that is,  $W^u(ISIS) = W^u(ISSI) = 0$ , and the interactions in the layers at even time can be arbitrary. We use the notation  $a = W^u(IISI)$ ,  $b'' = W^u(ISSI)$ ,  $c = W^u(ISSI)$  for the Boltzmann weight in the layers at even time (green boxes in Eq. (S200)). In terms of the entangling power  $e_u$  and the gate typically  $g_u$ , we have  $a = \frac{d}{d^2-1}e_u$ ,  $b = 1 - \frac{d^2+1}{2(d^2-1)}e_u - g_u$ , and  $c = -\frac{d^2+1}{2(d^2-1)}e_u + g_u$ . To exclude trivial examples, we assume that  $u$  is not locally equivalent to the identity gate, namely,  $e_u \neq 0$  and  $g_u \neq 0$ .

For technical simplicity, we apply the layer of Haar unitaries at the end of the circuit. Then, the frame potential can be written in terms of the transfer matrix  $T$  as follows:

$$T_{\sigma_1, \sigma_2, \dots, \sigma_n}^{\tau_1, \tau_2, \dots, \tau_n} = \begin{array}{c} \tau_1 \quad \tau_2 \quad \dots \quad \tau_n \\ \textcircled{\sigma_1} \textcircled{\sigma_2} \dots \textcircled{\sigma_n} \end{array} \quad (\text{S200})$$

where we have rotated the expression by 90 degrees, and the spins (balls) with gray color are summed over,  $\sigma_i, \tau_i \in \{I, S\}$ , and we obtain

$$F^{(2)} = \text{Tr}(T^{2t}). \quad (\text{S201})$$

Now, the problem of computing the frame potential reduces to computing the eigenvalues of the transfer matrix  $T$ . The leading eigenvalues are 1 and the corresponding eigenvectors are zero domain-wall configurations, namely,

$$T|I\rangle^{\otimes n} = |I\rangle^{\otimes n}, \quad (\text{S202})$$

$$T|S\rangle^{\otimes n} = |S\rangle^{\otimes n}. \quad (\text{S203})$$

To obtain the next-leading terms, we consider the transfer matrix  $T$  restricted to the subspace spanned by single domain-wall sector  $S_1 = \text{span}\{|i\rangle\}_{i=1}^{n-1}$ , where we have defined  $|i\rangle = |I\rangle^{\otimes i} \otimes |S\rangle^{\otimes n-i}$ , and we diagonalize the matrix in the subspace. We note that the diagonalization for Haar random brick-wall circuits is obtained in Ref. [86], and we extend the result to structured random brick-wall circuits. In the subspace, the  $I$ -type domain is always left side of the  $S$ -type domain, and the other subspace,

where the  $S$ -type domain is left to the  $I$ -type can be treated in the same way. The diagonal element  $\langle i|T|i\rangle$  can be obtained by summing the four domain wall configurations as follows:

$$\text{Diagram (S204)} \quad (S204)$$

where the black ball is  $I$  and the white ball  $S$ , and it implies

$$\begin{aligned} \langle i|T|i\rangle &= b'' + \frac{d}{d^2+1}a + \frac{d}{d^2+1}a + \left(\frac{d}{d^2+1}\right)^2 c \\ &= 1 - \frac{e_u + 2g_u}{2(d^2+1)^2(d^2-1)}d^6 - \frac{e_u - 2g_u}{2(d^2+1)^2(d^2-1)} \\ &= 1 - \frac{d^4 - d^2 + 1}{2(d^4-1)}e_u - \frac{d^4 + d^2 + 1}{(d^2+1)^2}g_u, \end{aligned} \quad (S205)$$

where in the first equality, we have used the equality  $W_H(IISI) = \frac{d}{d^2+1}$ . The off-diagonal elements in the single-domain wall subspace are nonzero only for  $\langle i|T|i+1\rangle$  and  $\langle i+1|T|i\rangle$  because a domain wall can move at most one site by one transfer matrix. Also, we have  $\langle i|T|i+1\rangle = \langle i+1|T|i\rangle$ . They are a sum of the two configurations as follows:

$$\text{Diagram (S206)} \quad (S206)$$

which implies

$$\begin{aligned} \langle i|T|i+1\rangle &= \frac{d}{d^2+1}a + \left(\frac{d}{d^2+1}\right)^2 c \\ &= \frac{d^4}{2(d^2+1)^2(d^2-1)}e_u + \frac{d^2}{(d^2+1)^2}g_u + \frac{d^2}{2(d^2+1)^2(d^2-1)}. \end{aligned} \quad (S207)$$

For most parameter regimes, the single domain-wall subspace is not an invariant subspace of  $T$ . Indeed, unless  $a = 0$  (where the two-qudit interaction  $V$  is either identity or SWAP up to single-qudit unitaries), the number of domain walls can increase by one at a boundary and increase by two in the bulk as the example configurations

$$\text{Diagram (S208)} \quad (S208)$$

Moreover, if there is more than one domain wall, unless  $c = 0$ , the number of domain walls can decrease at a boundary, for example,

$$\text{Diagram (S209)} \quad (S209)$$

We first consider the solvable condition  $c = 0$  and later discuss the general case. As we have explained in Sec. S3B, the condition is  $g_u = \frac{d^2+1}{2(d^2-1)}e_u$ . When  $c = 0$ , the number of domain walls can only increase, but such configurations do not contribute to the frame potential. This is because the frame potential is the trace of  $T^{2t}$ , and the initial and final spin configurations have to be the same, and therefore the number of domain wall is the same for all time. Then, it suffices to consider  $T$  restricted to the single domain wall subspace to obtain the leading eigenvalues. Let  $P_1$  be the projector onto the

subspace  $S_1$ . Then, we have

$$\begin{aligned}
P_1 T P_1 &= \left( \frac{2d \cdot a}{d^2 + 1} + b \right) \sum_{i=1}^{n-1} |i\rangle \langle i| + \frac{d \cdot a}{d^2 + 1} \sum_{i=1}^{n-2} (|i\rangle \langle i+1| + |i+1\rangle \langle i|) \\
&= \left( 1 - \frac{d^2 - 1}{2(d^2 + 1)} e_u - g_u \right) \sum_{i=1}^{n-1} |i\rangle \langle i| + \frac{d^2}{d^4 - 1} e_u \sum_{i=1}^{n-2} (|i\rangle \langle i+1| + |i+1\rangle \langle i|) \\
&= \left( 1 - \frac{d^4 + 1}{d^4 - 1} e_u \right) \sum_{i=1}^{n-1} |i\rangle \langle i| + \frac{d^2}{d^4 - 1} e_u \sum_{i=1}^{n-2} (|i\rangle \langle i+1| + |i+1\rangle \langle i|).
\end{aligned} \tag{S210}$$

The last equation above is a Hamiltonian of the tight-binding model with open boundary condition, and for  $k = 1, 2, \dots, n-1$ , the eigenvalues  $\lambda_k$  and eigenvectors  $|\phi_k\rangle$  are

$$\lambda_k = 1 - \frac{d^4 + 1}{d^4 - 1} e_u + \frac{d^2}{d^4 - 1} e_u \cos \frac{k\pi}{n}, \tag{S211}$$

$$|\phi_k\rangle = \sum_{i=1}^{n-1} \sin \frac{ki\pi}{n} |i\rangle. \tag{S212}$$

The second-largest eigenvalue is  $1 - \frac{d^4 + 1}{d^4 - 1} e_u + \frac{d^2}{d^4 - 1} e_u \cos \frac{\pi}{n}$ , and it becomes small when  $e_u$  is large. This is a rough reason why large  $e_u$  makes the frame potential smaller than the case of Haar random gates. For the case of Haar random gates, the eigenvalues are not the same as those in Sec. S4, where we have considered the periodic boundary condition, because in this section we consider the open boundary condition.

We define  $x = 1 - \frac{d^4 + 1}{d^4 - 1} e_u$  and  $y = \frac{d^2}{d^4 - 1} e_u$ . The contribution of single domain-wall configurations to the frame potential, which we denote by  $f_1$ , is

$$\begin{aligned}
f_1 &= \sum_{k=1}^{n-1} \lambda_k^{2t} \\
&= \sum_{k=1}^{n-1} \sum_{i=1}^{2t} \binom{2t}{i} x^{2t-i} y^i \cos^i \left( \frac{k\pi}{n} \right) \\
&= \sum_{k=1}^{n-1} \sum_{i=1}^t \binom{2t}{2i} x^{2t-2i} y^{2i} \cos^{2i} \left( \frac{k\pi}{n} \right) \\
&= \sum_{i=1}^t \binom{2t}{2i} x^{2t-2i} y^{2i} \left( \frac{n}{4^i} \sum_{k=-\lfloor i/n \rfloor}^{\lfloor i/n \rfloor} \binom{2i}{i+kn} - 1 \right) \\
&= n \sum_{k=-\lfloor t/n \rfloor}^{\lfloor t/n \rfloor} \sum_{i=kn}^t \binom{2t}{2i} \binom{2i}{i+kn} \frac{x^{2t-2i} y^{2i}}{4^i} - \frac{1}{2} ((x+y)^t + (x-y)^t) \\
&= nx^{2t} \sum_{k=-\lfloor t/n \rfloor}^{\lfloor t/n \rfloor} \left( \frac{y}{2x} \right)^{2kn} {}_2F_1 \left[ \begin{matrix} t - kn, t - kn - \frac{1}{2}, \frac{y^2}{x^2} \\ 1 + 2kn \end{matrix}; \frac{y^2}{x^2} \right] - \frac{1}{2} ((x+y)^t + (x-y)^t)
\end{aligned} \tag{S213}$$

where we have used the equalities  $\sum_{k=1}^{n-1} \cos^{2i+1} \left( \frac{k\pi}{n} \right) = 0$  and  $\sum_{k=0}^{n-1} \cos^{2i} \left( \frac{k\pi}{n} \right) = \frac{n}{4^i} \sum_{k=-\lfloor i/n \rfloor}^{\lfloor i/n \rfloor} \binom{2i}{i+kn}$  for an integer  $i$  [87], and

$${}_2F_1 \left[ \begin{matrix} a, b \\ c \end{matrix}; z \right] = \sum_{i=0}^{\infty} \frac{(a)_n (b)_n}{(c)_n} z^i, \quad (a)_n = \prod_{j=0}^{n-1} (a+j), \tag{S214}$$

is the hypergeometric function. These single domain-wall configurations contribute to the frame potential dominantly, and from the above expression, we find that the contributions become small when  $e_u$  is large.

We give a non-rigorous but intuitive argument for the value of the frame potential for non-zero  $c$ , and we show that the single-domain calculation is not a good approximation for  $c \neq 0$  for  $\Omega(n)$ -depth. When  $c \neq 0$ , spin configurations without conserving the number of domain walls can have nonzero value. As we discuss below, if  $t$  is much greater than  $n$ , violation

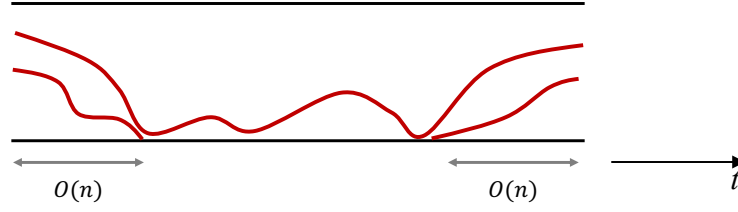


FIG. S3. Non-conservation of the number of domain walls.

of the conservation of the number of the domain wall should increase the frame potential compared to the case  $c = 0$ . The weight of the spin configurations with domain walls roughly decays exponentially in the total length of domain walls. If there are domain walls  $k$  and the number is conserved, then the total length is  $\Omega(kt)$ , and the weight is  $O(e^{-kt})$ . However, if the number does not conserve (for example, Fig. S3), the domain-wall number can be one after  $O(n)$  time steps, and the dominant weight of configurations starting from  $k$  domain-walls is only  $O(e^{-2nk-(t-2n)}) = O(e^{-t})$ .

### S7. DIAGONALIZATION OF $\mathcal{M}_k$

We note that, from Eqs. (S162) and (S163),  $\mathcal{S}_{2,k} = P\mathcal{S}_{1,k}P$  with  $P = \text{diag}(1, 1, -1, -1)$ , which implies

$$\mathcal{M}_k = (Pe^{\mathcal{S}_{1,k}})^2. \quad (\text{S215})$$

Thus, it is sufficient to diagonalize  $Pe^{\mathcal{S}_{1,k}}$ .  $\mathcal{S}_{1,k}$  is written as

$$\mathcal{S}_{1,k} = \begin{pmatrix} A & B \\ -B & C \end{pmatrix} \quad (\text{S216})$$

with

$$A = \frac{1}{2} \begin{pmatrix} 2x + y \cos k & -i(2x + y) \sin k \\ -i(2x - y) \sin k & -2x - y \cos k \end{pmatrix}, \quad (\text{S217})$$

$$B = \frac{1}{2} \begin{pmatrix} -iy \sin k & (2x + y) \cos k \\ (2x - y) \cos k & iy \sin k \end{pmatrix}, \quad (\text{S218})$$

$$C = \frac{1}{2} \begin{pmatrix} 2x - y \cos k & i(2x + y) \sin k \\ i(2x - y) \sin k & -2x + y \cos k \end{pmatrix}. \quad (\text{S219})$$

We define

$$\mathbf{u}_1 = \begin{pmatrix} (y + 2x) \cos(\frac{k}{2}) \\ i(y - 2x) \sin(\frac{k}{2}) \end{pmatrix}, \quad \mathbf{u}_2 = \begin{pmatrix} i \sin(\frac{k}{2}) \\ \cos(\frac{k}{2}) \end{pmatrix}, \quad \mathbf{v}_1 = \begin{pmatrix} i(y + 2x) \sin(\frac{k}{2}) \\ (y - 2x) \cos(\frac{k}{2}) \end{pmatrix}, \quad \mathbf{v}_2 = \begin{pmatrix} \cos(\frac{k}{2}) \\ i \sin(\frac{k}{2}) \end{pmatrix}, \quad (\text{S220})$$

where  $\mathbf{u}_1$  and  $\mathbf{u}_2$  are the eigenvectors of  $A$  and  $\mathbf{v}_1$  and  $\mathbf{v}_2$  are the eigenvectors of  $C$ . These vectors satisfy

$$A\mathbf{u}_1 = \frac{1}{2}(y + 2x \cos k)\mathbf{u}_1, \quad A\mathbf{u}_2 = -\frac{1}{2}(y + 2x \cos k)\mathbf{u}_2, \quad (\text{S221})$$

$$-B\mathbf{u}_1 = \frac{1}{2}(y + 2x \cos k)\mathbf{v}_1, \quad -B\mathbf{u}_2 = -\frac{1}{2}(y + 2x \cos k)\mathbf{v}_2, \quad (\text{S222})$$

$$B\mathbf{v}_1 = \frac{1}{2}(y - 2x \cos k)\mathbf{u}_1, \quad B\mathbf{v}_2 = -\frac{1}{2}(y - 2x \cos k)\mathbf{u}_2, \quad (\text{S223})$$

$$C\mathbf{v}_1 = \frac{1}{2}(y - 2x \cos k)\mathbf{v}_1, \quad C\mathbf{v}_2 = -\frac{1}{2}(y - 2x \cos k)\mathbf{v}_2, \quad (\text{S224})$$

which implies

$$\begin{pmatrix} \mathbf{u}_1 & \mathbf{u}_2 \\ \mathbf{v}_1 & \mathbf{v}_2 \end{pmatrix}^{-1} \begin{pmatrix} A & B \\ -B & C \end{pmatrix} \begin{pmatrix} \mathbf{u}_1 & \mathbf{u}_2 \\ \mathbf{v}_1 & \mathbf{v}_2 \end{pmatrix} = \begin{pmatrix} D & \\ & -D \end{pmatrix} \quad (\text{S225})$$

with

$$D := \frac{1}{2} \begin{pmatrix} y + 2x \cos k & y - 2x \cos k \\ y + 2x \cos k & y - 2x \cos k \end{pmatrix}. \quad (\text{S226})$$

We also have

$$\begin{pmatrix} \mathbf{u}_1 & \mathbf{u}_2 \\ \mathbf{v}_1 & \mathbf{v}_2 \end{pmatrix}^{-1} P \begin{pmatrix} \mathbf{u}_1 & \mathbf{u}_2 \\ \mathbf{v}_1 & \mathbf{v}_2 \end{pmatrix} = \begin{pmatrix} Z & \\ & Z \end{pmatrix}. \quad (\text{S227})$$

By Eqs. (S216), (S225), and (S227), we get

$$\begin{pmatrix} \mathbf{u}_1 & \mathbf{u}_2 \\ \mathbf{v}_1 & \mathbf{v}_2 \end{pmatrix}^{-1} P e^{S_{1,k}} \begin{pmatrix} \mathbf{u}_1 & \mathbf{u}_2 \\ \mathbf{v}_1 & \mathbf{v}_2 \end{pmatrix} = \begin{pmatrix} Z e^D & \\ & Z e^{-D} \end{pmatrix}. \quad (\text{S228})$$

By a straightforward calculation, we find

$$\begin{aligned} Z e^D &= e^{\frac{y}{2}} \begin{pmatrix} \cosh\left(\frac{y}{2}\right) + q_k & \sinh\left(\frac{y}{2}\right) - q_k \\ -\sinh\left(\frac{y}{2}\right) - q_k & -\cosh\left(\frac{y}{2}\right) + q_k \end{pmatrix} \\ &= \begin{pmatrix} \cosh\left(\frac{y+2\beta}{4}\right) & -\sinh\left(\frac{y-2\beta}{4}\right) \\ -\sinh\left(\frac{y+2\beta}{4}\right) & \cosh\left(\frac{y-2\beta}{4}\right) \end{pmatrix} \begin{pmatrix} e^{\frac{y+2\beta}{2}} & \\ & -e^{\frac{y-2\beta}{2}} \end{pmatrix} \begin{pmatrix} \cosh\left(\frac{y+2\beta}{4}\right) & -\sinh\left(\frac{y-2\beta}{4}\right) \\ -\sinh\left(\frac{y+2\beta}{4}\right) & \cosh\left(\frac{y-2\beta}{4}\right) \end{pmatrix}^{-1} \end{aligned} \quad (\text{S229})$$

with  $q_k := x \cos k \sinh(y/2)/(y/2)$  and  $\beta := \sinh^{-1} q_k$ . By substituting  $x \mapsto -x$  and  $y \mapsto -y$  in Eq. (S229), we get

$$Z e^{-D} = \begin{pmatrix} \cosh\left(\frac{y+2\beta}{4}\right) & \sinh\left(\frac{y-2\beta}{4}\right) \\ \sinh\left(\frac{y+2\beta}{4}\right) & \cosh\left(\frac{y-2\beta}{4}\right) \end{pmatrix} \begin{pmatrix} e^{-\frac{y-2\beta}{2}} & \\ & -e^{\frac{-y+2\beta}{2}} \end{pmatrix} \begin{pmatrix} \cosh\left(\frac{y+2\beta}{4}\right) & \sinh\left(\frac{y-2\beta}{4}\right) \\ \sinh\left(\frac{y+2\beta}{4}\right) & \cosh\left(\frac{y-2\beta}{4}\right) \end{pmatrix}^{-1}. \quad (\text{S230})$$

By Eqs. (S215), (S216), (S228), (S229), and (S230), we get

$$\mathcal{M}_k = E \begin{pmatrix} e^{y+2\beta} & & & \\ & e^{y-2\beta} & & \\ & & e^{-y-2\beta} & \\ & & & e^{-y+2\beta} \end{pmatrix} E^{-1} \quad (\text{S231})$$

with

$$\begin{aligned} E &:= \begin{pmatrix} \mathbf{u}_1 & \mathbf{u}_2 \\ \mathbf{v}_1 & \mathbf{v}_2 \end{pmatrix} \begin{pmatrix} \cosh\left(\frac{y+2\beta}{4}\right) & -\sinh\left(\frac{y-2\beta}{4}\right) & & \\ -\sinh\left(\frac{y+2\beta}{4}\right) & \cosh\left(\frac{y-2\beta}{4}\right) & & \\ & & \cosh\left(\frac{y+2\beta}{4}\right) & \sinh\left(\frac{y-2\beta}{4}\right) \\ & & \sinh\left(\frac{y+2\beta}{4}\right) & \cosh\left(\frac{y-2\beta}{4}\right) \end{pmatrix} \\ &= \begin{pmatrix} (y+2x) \cos\left(\frac{k}{2}\right) \cosh\left(\frac{y+2\beta}{4}\right) & -(y+2x) \cos\left(\frac{k}{2}\right) \sinh\left(\frac{y-2\beta}{4}\right) & i \sin\left(\frac{k}{2}\right) \cosh\left(\frac{y+2\beta}{4}\right) & i \sin\left(\frac{k}{2}\right) \sinh\left(\frac{y-2\beta}{4}\right) \\ i(y-2x) \sin\left(\frac{k}{2}\right) \cosh\left(\frac{y+2\beta}{4}\right) & -i(y-2x) \sin\left(\frac{k}{2}\right) \sinh\left(\frac{y-2\beta}{4}\right) & \cos\left(\frac{k}{2}\right) \cosh\left(\frac{y+2\beta}{4}\right) & \cos\left(\frac{k}{2}\right) \sinh\left(\frac{y-2\beta}{4}\right) \\ -i(y+2x) \sin\left(\frac{k}{2}\right) \sinh\left(\frac{y+2\beta}{4}\right) & i(y+2x) \sin\left(\frac{k}{2}\right) \cosh\left(\frac{y-2\beta}{4}\right) & \cos\left(\frac{k}{2}\right) \sinh\left(\frac{y+2\beta}{4}\right) & \cos\left(\frac{k}{2}\right) \cosh\left(\frac{y-2\beta}{4}\right) \\ -(y-2x) \cos\left(\frac{k}{2}\right) \sinh\left(\frac{y+2\beta}{4}\right) & (y-2x) \cos\left(\frac{k}{2}\right) \cosh\left(\frac{y-2\beta}{4}\right) & i \sin\left(\frac{k}{2}\right) \sinh\left(\frac{y+2\beta}{4}\right) & i \sin\left(\frac{k}{2}\right) \cosh\left(\frac{y-2\beta}{4}\right) \end{pmatrix}. \end{aligned} \quad (\text{S232})$$

With the equality  $e^\beta = q_k + \sqrt{1 + q_k^2}$  and the modification for the diagonalizing matrix  $E$  by dividing each column of it by the top element of the column, we obtain the diagonalization in Sec. S5 B 1.



- [2] E. Knill, D. Leibfried, R. Reichle, J. Britton, R. B. Blakestad, J. D. Jost, C. Langer, R. Ozeri, S. Seidelin, and D. J. Wineland, Randomized benchmarking of quantum gates, *Phys. Rev. A* **77**, 012307 (2008).
- [3] E. Magesan, J. M. Gambetta, and J. Emerson, Scalable and robust randomized benchmarking of quantum processes, *Phys. Rev. Lett.* **106**, 180504 (2011).
- [4] J. Eisert, D. Hangleiter, N. Walk, I. Roth, D. Markham, R. Parekh, U. Chabaud, and E. Kashefi, Quantum certification and benchmarking, *Nature Rev. Phys.* **2**, 382 (2020).
- [5] S. Boixo, S. V. Isakov, V. N. Smelyanskiy, R. Babbush, N. Ding, Z. Jiang, M. J. Bremner, J. M. Martinis, and H. Neven, Characterizing quantum supremacy in near-term devices, *Nature Phys.* **14**, 595 (2018).
- [6] F. Arute *et al.*, Quantum supremacy using a programmable superconducting processor, *Nature* **574**, 505 (2019).
- [7] B. Ware, A. Deshpande, D. Hangleiter, P. Niroula, B. Fefferman, A. V. Gorshkov, and M. J. Gullans, A sharp phase transition in linear cross-entropy benchmarking (2023), [arXiv:2305.04954](https://arxiv.org/abs/2305.04954).
- [8] A. Morvan, B. Villalonga, X. Mi, S. Mandra, A. Bengtsson, P. Klimov, Z. Chen, S. Hong, C. Erickson, I. Drozdov, *et al.*, Phase transition in random circuit sampling (2023), [arXiv:2304.11119](https://arxiv.org/abs/2304.11119).
- [9] B. Fefferman, S. Ghosh, and W. Zhan, Anti-concentration for the unitary Haar measure and applications to random quantum circuits (2024), [arXiv:2407.19561](https://arxiv.org/abs/2407.19561).
- [10] D. Hangleiter and J. Eisert, Computational advantage of quantum random sampling, *Rev. Mod. Phys.* **95**, 035001 (2023).
- [11] H.-Y. Huang, R. Kueng, and J. Preskill, Predicting many properties of a quantum system from very few measurements, *Nature Phys.* **16**, 1050 (2020).
- [12] A. Zhao, N. C. Rubin, and A. Miyake, Fermionic partial tomography via classical shadows, *Phys. Rev. Lett.* **127**, 110504 (2021).
- [13] A. Elben, S. T. Flammia, H.-Y. Huang, R. Kueng, J. Preskill, B. Vermersch, and P. Zoller, The randomized measurement toolbox, *Nature Rev. Phys.* **5**, 9 (2023).
- [14] C. Bertoni, J. Haferkamp, M. Hinsche, M. Ioannou, J. Eisert, and H. Pashayan, Shallow shadows: Expectation estimation using low-depth random clifford circuits, *Phys. Rev. Lett.* **133**, 020602 (2024).
- [15] K. Wan, W. J. Huggins, J. Lee, and R. Babbush, Matchgate shadows for fermionic quantum simulation, *Comm. Math. Phys.* **404**, 629 (2023).
- [16] A. Nahum, S. Vijay, and J. Haah, Operator spreading in random unitary circuits, *Phys. Rev. X* **8**, 021014 (2018).
- [17] A. Nahum, J. Ruhman, S. Vijay, and J. Haah, Quantum entanglement growth under random unitary dynamics, *Phys. Rev. X* **7**, 031016 (2017).
- [18] P. Hosur, X.-L. Qi, D. A. Roberts, and B. Yoshida, Chaos in quantum channels, *JHEP* **2016**, 1.
- [19] D. A. Roberts and B. Yoshida, Chaos and complexity by design, *JHEP* **2017**, 1.
- [20] F. G. Brandão, W. Chemissany, N. Hunter-Jones, R. Kueng, and J. Preskill, Models of quantum complexity growth, *PRX Quantum* **2**, 030316 (2021).
- [21] J. Haferkamp, P. Faist, N. B. T. Kothakonda, J. Eisert, and N. Yunger Halpern, Linear growth of quantum circuit complexity, *Nature Phys.* **18**, 528 (2022).
- [22] R. Suzuki, J. Haferkamp, J. Eisert, and P. Faist, Quantum complexity phase transitions in monitored random circuits (2023), [arXiv:2305.15475](https://arxiv.org/abs/2305.15475).
- [23] M. P. Fisher, V. Khemani, A. Nahum, and S. Vijay, Random quantum circuits, *Ann. Rev. Cond. Matt. Phys.* **14**, 335 (2023).
- [24] A. W. Harrow and R. A. Low, Random quantum circuits are approximate 2-designs, *Comm. Math. Phys.* **291**, 257 (2009).
- [25] F. G. Brandao, A. W. Harrow, and M. Horodecki, Local random quantum circuits are approximate polynomial-designs, *Comm. Math. Phys.* **346**, 397 (2016).
- [26] S. Mittal and N. Hunter-Jones, Local random quantum circuits form approximate designs on arbitrary architectures (2023), [arXiv:2310.19355](https://arxiv.org/abs/2310.19355).
- [27] D. Belkin, J. Allen, S. Ghosh, C. Kang, S. Lin, J. Sud, F. Chong, B. Fefferman, and B. K. Clark, Approximate  $t$ -designs in generic circuit architectures (2023), [arXiv:2310.19783](https://arxiv.org/abs/2310.19783).
- [28] C.-F. Chen, J. Haah, J. Haferkamp, Y. Liu, T. Metger, and X. Tan, Incompressibility and spectral gaps of random circuits (2024), [arXiv:2406.07478](https://arxiv.org/abs/2406.07478).
- [29] A. E. Deneris, P. Bermejo, P. Braccia, L. Cincio, and M. Cerezo, Exact spectral gaps of random one-dimensional quantum circuits (2024), [arXiv:2408.11201](https://arxiv.org/abs/2408.11201).
- [30] I. Marvian, Restrictions on realizable unitary operations imposed by symmetry and locality, *Nature Phys.* **18**, 283 (2022).
- [31] Y. Mitsuhashi, R. Suzuki, T. Soejima, and N. Yoshioka, Unitary designs of symmetric local random circuits (2024), [arXiv:2408.13472](https://arxiv.org/abs/2408.13472).
- [32] Y. Mitsuhashi, R. Suzuki, T. Soejima, and N. Yoshioka, Characterization of randomness in quantum circuits of continuous gate sets (2024), [arXiv:2408.13475](https://arxiv.org/abs/2408.13475).
- [33] A. Hulse, H. Liu, and I. Marvian, Unitary designs from random symmetric quantum circuits (2024), [arXiv:2408.14463](https://arxiv.org/abs/2408.14463).
- [34] Y. Nakata, C. Hirche, M. Koashi, and A. Winter, Efficient quantum pseudorandomness with nearly time-independent Hamiltonian dynamics, *Phys. Rev. X* **7**, 021006 (2017).
- [35] E. Onorati, O. Buijsscher, M. Kliesch, W. Brown, A. H. Werner, and J. Eisert, Mixing properties of stochastic quantum Hamiltonians, *Commun. Math. Phys.* **355**, 905 (2017).
- [36] J. Haferkamp, Random quantum circuits are approximate unitary  $t$ -designs in depth  $O(nt^{5+o(1)})$ , *Quantum* **6**, 795 (2022).
- [37] A. Deshpande, P. Niroula, O. Shtanko, A. V. Gorshkov, B. Fefferman, and M. J. Gullans, Tight bounds on the convergence of noisy random circuits to the uniform distribution, *PRX Quantum* **3**, 040329 (2022).
- [38] A. W. Harrow and S. Mehraban, Approximate unitary  $t$ -designs by short random quantum circuits using nearest-neighbor and long-range gates, *Comm. Math. Phys.* **401**, 1531 (2023).
- [39] T. Schuster, J. Haferkamp, and H.-Y. Huang, Random unitaries in extremely low depth (2024), [arXiv:2407.07754](https://arxiv.org/abs/2407.07754).
- [40] N. LaRacuente and F. Leditzky, Approximate unitary  $k$ -designs from shallow, low-communication circuits (2024), [arXiv:2407.07876](https://arxiv.org/abs/2407.07876).

- [41] D. Gross, K. Audenaert, and J. Eisert, Evenly distributed unitaries: On the structure of unitary designs, *J. Math. Phys.* **48**, 052104 (2007).
- [42] A. B. Watts, D. Gosset, Y. Liu, and M. Soleimanifar, Quantum advantage from measurement-induced entanglement in random shallow circuits (2024), [arXiv:2407.21203](https://arxiv.org/abs/2407.21203).
- [43] J. Haferkamp, On the moments of random quantum circuits and robust quantum complexity (2023), [arXiv:2303.16944](https://arxiv.org/abs/2303.16944).
- [44] M. Heinrich, M. Kliesch, and I. Roth, Randomized benchmarking with random quantum circuits (2022), [arXiv:2212.06181](https://arxiv.org/abs/2212.06181).
- [45] C. Bertoni, J. Haferkamp, M. Hinsche, M. Ioannou, J. Eisert, and H. Pashayan, Shallow shadows: Expectation estimation using low-depth random clifford circuits, *Phys. Rev. Lett.* **133**, 020602 (2024).
- [46] This first layer becomes unimportant when we consider a sufficiently large depth  $\Omega(n)$ , because of the left- and right-invariance of the Haar random unitaries.
- [47] See Supplementary Materials for more details (URL to be added).
- [48] C. Dankert, R. Cleve, J. Emerson, and E. Livine, Exact and approximate unitary 2-designs and their application to fidelity estimation, *Phys. Rev. A* **80**, 012304 (2009).
- [49] Á. Kaposi, Z. Kolarovszki, A. Solymos, and Z. Zimborás, Generalized group designs: overcoming the 4-design-barrier and constructing novel unitary 2-designs in arbitrary dimensions (2024), [arXiv:2405.00919](https://arxiv.org/abs/2405.00919).
- [50] R. Bhatia, *Matrix analysis*, Vol. 169 (Springer Science & Business Media, 2013).
- [51] R. A. Low, Large deviation bounds for k-designs, *Proc. Roy. Soc. A* **465**, 3289 (2009).
- [52] J. Haferkamp, C. Bertoni, I. Roth, and J. Eisert, Emergent statistical mechanics from properties of disordered random matrix product states, *PRX Quantum* **2**, 040308 (2021).
- [53] P. Zanardi, C. Zalka, and L. Faoro, Entangling power of quantum evolutions, *Phys. Rev. A* **62**, 030301 (2000).
- [54] B. Jonnadula, P. Mandayam, K. Życzkowski, and A. Lakshminarayan, Impact of local dynamics on entangling power, *Phys. Rev. A* **95**, 040302 (2017).
- [55] B. Jonnadula, P. Mandayam, K. Życzkowski, and A. Lakshminarayan, Entanglement measures of bipartite quantum gates and their thermalization under arbitrary interaction strength, *Phys. Rev. Res.* **2**, 043126 (2020).
- [56] S. Aravinda, S. A. Rather, and A. Lakshminarayan, From dual-unitary to quantum Bernoulli circuits: Role of the entangling power in constructing a quantum ergodic hierarchy, *Phys. Rev. Res.* **3**, 043034 (2021).
- [57] L. G. Valiant, Quantum computers that can be simulated classically in polynomial time, in *Proceedings of the Thirty-Third Annual ACM Symposium on Theory of Computing*, STOC '01 (Association for Computing Machinery, New York, NY, USA, 2001) p. 114–123.
- [58] B. M. Terhal and D. P. DiVincenzo, Classical simulation of noninteracting-fermion quantum circuits, *Phys. Rev. A* **65**, 032325 (2002).
- [59] R. Jozsa and A. Miyake, Matchgates and classical simulation of quantum circuits, *Proc. Roy. Soc. A* **464**, 3089 (2008).
- [60] A. Y. Kitaev, Unpaired majorana fermions in quantum wires, *Physics-Uspekhi* **44**, 131 (2001).
- [61] B. Bertini, P. Kos, and T. Prosen, Exact correlation functions for dual-unitary lattice models in 1+1 dimensions, *Phys. Rev. Lett.* **123**, 210601 (2019).
- [62] L. Piroli, B. Bertini, J. I. Cirac, and T. Prosen, Exact dynamics in dual-unitary quantum circuits, *Phys. Rev. B* **101**, 094304 (2020).
- [63] P. W. Claeys and A. Lamacraft, Ergodic and nonergodic dual-unitary quantum circuits with arbitrary local hilbert space dimension, *Phys. Rev. Lett.* **126**, 100603 (2021).
- [64] R. Suzuki, K. Mitarai, and K. Fujii, Computational power of one-and two-dimensional dual-unitary quantum circuits, *Quantum* **6**, 631 (2022).
- [65] D. Hangleiter, J. Bermejo-Vega, M. Schwarz, and J. Eisert, Anticoncentration theorems for schemes showing a quantum speedup, *Quantum* **2**, 65 (2018).
- [66] A. M. Dalzell, N. Hunter-Jones, and F. G. S. L. Brandão, Random quantum circuits anticoncentrate in log depth, *PRX Quantum* **3**, 010333 (2022).
- [67] A. Roy and A. J. Scott, Unitary designs and codes, *Des. Code. Crypt.* **53**, 13 (2009).
- [68] M. J. Gullans, S. Krastanov, D. A. Huse, L. Jiang, and S. T. Flammia, Quantum coding with low-depth random circuits, *Phys. Rev. X* **11**, 031066 (2021).
- [69] J. Bae, B. C. Hiesmayr, and D. McNulty, Linking entanglement detection and state tomography via quantum 2-designs, *New J. Phys.* **21**, 013012 (2019).
- [70] T. Zhou and D. J. Luitz, Operator entanglement entropy of the time evolution operator in chaotic systems, *Phys. Rev. B* **95**, 094206 (2017).
- [71] P. Richelli, K. Schoutens, and A. Zorzato, Brick wall quantum circuits with global fermionic symmetry, *SciPost Physics* **17**, 087 (2024).
- [72] S.-K. Jian, G. Bentsen, and B. Swingle, Linear growth of circuit complexity from Brownian dynamics, *JHEP* **2023**, 1.
- [73] M. Žnidarič, Exact convergence times for generation of random bipartite entanglement, *Phys. Rev. A* **78**, 032324 (2008).
- [74] R. A. Horn and C. R. Johnson, *Matrix analysis* (Cambridge University Press, 2012).
- [75] M. A. Graydon, J. Skanes-Norman, and J. J. Wallman, Clifford groups are not always 2-designs (2021), [arXiv:2108.04200](https://arxiv.org/abs/2108.04200).
- [76] B. Collins and P. Śniady, Integration with respect to the Haar measure on unitary, orthogonal and symplectic group, *Comm. Math. Phys.* **264**, 773 (2006).
- [77] J. Eisert, Entangling power and quantum circuit complexity, *Phys. Rev. Lett.* **127**, 020501 (2021).
- [78] T. Prosen and I. Pižorn, Operator space entanglement entropy in a transverse ising chain, *Phys. Rev. A* **76**, 032316 (2007).
- [79] F. Pastawski, B. Yoshida, D. Harlow, and J. Preskill, Holographic quantum error-correcting codes: Toy models for the bulk/boundary correspondence, *JHEP* **2015**, 1.
- [80] D. Goyeneche, D. Alsina, J. I. Latorre, A. Riera, and K. Życzkowski, Absolutely maximally entangled states, combinatorial designs, and multiunitary matrices, *Phys. Rev. A* **92**, 032316 (2015).
- [81] N. Hunter-Jones, Unitary designs from statistical mechanics in random quantum circuits (2019), [arXiv:1905.12053](https://arxiv.org/abs/1905.12053).
- [82] S. Vardhan and S. Moudgalya, Entanglement dynamics from universal low-lying modes (2024), [arXiv:2407.16763](https://arxiv.org/abs/2407.16763).

- [83] H. Katsura, D. Schuricht, and M. Takahashi, Exact ground states and topological order in interacting Kitaev/Majorana chains, *Phys. Rev. B* **92**, 115137 (2015).
- [84] J. Wouters, H. Katsura, and D. Schuricht, Exact ground states for interacting Kitaev chains, *Phys. Rev. B* **98**, 155119 (2018).
- [85] T. Zhou and A. Nahum, Emergent statistical mechanics of entanglement in random unitary circuits, *Phys. Rev. B* **99**, 174205 (2019).
- [86] M. A. Rampp and P. W. Claeys, Hayden-Preskill recovery in chaotic and integrable unitary circuit dynamics, *Quantum* **8**, 1434 (2024).
- [87] M. Merca, On some power sums of sine or cosine, *Am. Math. Mon.* **121**, 244 (2014).